REPORT 1268

THEORETICAL CALCULATIONS OF THE PRESSURES, FORCES, AND MOMENTS AT SUPERSONIC SPEEDS DUE TO VARIOUS LATERAL MOTIONS ACTING ON THIN ISOLATED VERTICAL TAILS [1]

By Kenneth Margolis and Percy J. Bobbitt

SUMMARY

Velocity potentials, pressure distributions, and stability derivatives are derived by use of supersonic linearized theory for families of thin isolated vertical tails performing steady rolling, steady yawing, and constant-lateral-acceleration motions. Vertical-tail families (half-delta and rectangular plan forms) are considered for a broad Mach number range. Also considered are the vertical tail with arbitrary sweepback and taper ratio at Mach numbers for which both the leading edge and trailing edge of the tail are supersonic and the triangular vertical tail with a subsonic leading edge and a supersonic trailing edge. For purposes of completeness, analogous expressions and derivatives for sideslip motion obtained primarily from other sources are included.

Expressions for potentials, pressures, and stability derivatives are tabulated. Curves which determine the stability derivatives for half-delta and rectangular tails are presented which enable rapid estimation of their values for given values of aspect ratio and Mach number. In order to indicate the importance of end-plate effects, several comparisons are shown of the derived results (based on a zero-end-plate analysis) with those corresponding to a complete-end-plate analysis.

INTRODUCTION

Detailed knowledge of the loading, forces, and moments acting on vertical tails undergoing various maneuvers is a necessary prerequisite for determining the lateral dynamic behavior of aircraft. The information presently available is, in many instances, insufficient to enable reliable estimates to be made of the vertical-tail contributions to airplane stability at supersonic speeds. Aside from calculations for several "slender" configurations, theoretical results to date have been concerned, for the most part, with tail configurations either subject to a constant sideslip attitude or performing a steady rolling motion (see refs. 1 to 13).

For the sideslip motion, the effects of Mach number and aspect ratio on the aerodynamic loads of a number of tail configurations with both one and two planes of cross-sectional symmetry have already been investigated extensively. The same effects on tail arrangements in a rolling motion

have also received considerable attention which has mainly been directed toward tails with two planes of symmetry such as cruciform arrangements. Additional theoretical analysis devoted to the evaluation of the Mach number and aspect-ratio effects on the forces and moments acting on tail systems in roll with one plane of cross-sectional symmetry is required. Tail arrangements performing a steady yawing motion or a constant-lateral-acceleration motion have received little attention to date in the literature. Yet the forces and moments produced by these motions are by no means negligible, and some indication of their magnitudes is necessary, particularly at supersonic speeds, in order to evaluate their relative importance on lateral stability.

The primary purpose of this report is to present the results of a theoretical investigation to determine at supersonic speeds the pressures, forces, and moments acting on several families of thin isolated vertical tails subject to various lateral disturbances. Three motions are treated: steady rolling, steady yawing, and constant lateral acceleration. A fourth motion, namely, constant sideslip, although analyzed previously, is included for purposes of completeness. The basic plan forms considered are: (a) half-delta tail with either a subsonic or supersonic leading edge, (b) rectangular tail, (c) general sweptback tail of arbitrary taper ratio with supersonic leading and trailing edges, and (d) triangular tail with a subsonic leading edge and a supersonic trailing edge. The half-delta and rectangular vertical tails are analyzed in detail in that forces and moments (expressed in the form of stability derivatives) and their variations with Mach number and aspect ratio are presented in a series of simple charts. Useful expressions and formulas are included for the other plan forms which enable similar calculations to be carried out.

A secondary objective, in view of the geometric nonplanar characteristics of tail arrangements, is to consider the estimation of the mutual aerodynamic interference that exists between the vertical and horizontal tails. In order to gain some insight into the possible effects of such interference, several of the derived results are compared with corresponding calculations based on a complete-end-plate analysis. (A complete-end-plate analysis implies that the horizontal tail acts as a perfect reflection plane.)

SYMBOLS

x,y,z rectangular coordinates used in analysis (see fig. 2(a))

$\theta=z/x$

ξ,ζ rectangular coordinates of doublet

$\sigma=\zeta/\xi$

x_0,z_0 longitudinal and vertical distances, respectively, that origin is displaced relative to tail apex (see fig. 2(c))

u,v perturbation velocities in x- and y-directions, respectively

V free-stream or flight velocity (see fig. 2)

M Mach number, V/Speed of sound

$B=\sqrt{M^2-1}$

p,r angular velocities about x- and z-axes, respectively (see fig. 2)

β angle of sideslip (see table I)

$\dot{\beta}$ rate of change of β with time, $d\beta/dt$

t time

ρ density of air

q free-stream dynamic pressure, $\frac{1}{2}\rho V^2$

$\Delta P/q$ coefficient of pressure difference between opposite sides of tail surface due to particular motion under consideration, positive in sense of positive side force (see fig. 2)

κ constant determining degree of homogeneity of quasi-conical velocity field

φ perturbation velocity potential due to particular motion under consideration evaluated on positive y-side of tail surface (see fig. 2)

$\Delta\varphi$ difference in perturbation velocity potential between two sides of tail surface, $\varphi(x,0^+,z)-\varphi(x,0^-,z)$

φ_D potential of supersonic doublet distribution

φ_L potential of line of doublets

$A(x,z)$ doublet-strength function

$f(\sigma)$ line-doublet-distribution function

c_r root chord of vertical tail

b span of vertical tail

S area of vertical tail

λ taper ratio of vertical tail, Tip chord/Root chord

A aspect ratio of vertical tail, b^2/S

m slope of leading edge of tail; cotangent of sweepback angle of leading edge (see fig.1)

$$k=\frac{1-\sqrt{1-B^2m^2}}{Bm}$$

$$H(Bm)=\frac{\sqrt{2(1-\sqrt{1-B^2m^2})}}{E'(k)}$$

$E'(k)$ complete elliptic integral of second kind with modulus $\sqrt{1-k^2}$,

$$\int_0^{\pi/2}\sqrt{1-(1-k^2)\sin^2 n}\,dn$$

$K'(k)$ complete elliptic integral of first kind with modulus $\sqrt{1-k^2}$,

$$\int_0^{\pi/2}\frac{dn}{\sqrt{1-(1-k^2)\sin^2 n}}$$

$\tau,\omega,\bar{\omega}$ arbitrary constants $(\bar{\omega}=\omega Bm)$

$$\tau_p'=-\frac{\sqrt{1+k^2}[k^2(1+k^2)K'(k)+(1-4k^2+k^4)E'(k)]}{(2-k^2)(1-2k^2)E'(k)^2+k^2(1+k^2)K'(k)E'(k)-k^4K'(k)^2}$$

$$\omega_p'=-\frac{(1+k^2)^{3/2}[(1+k^2)E'(k)-2k^2K'(k)]}{2[(2-k^2)(1-2k^2)E'(k)^2+k^2(1+k^2)K'(k)E'(k)-k^4K'(k)^2]}$$

$$\tau_r'=-\frac{k\sqrt{1+k^2}[(1+k^2)E'(k)-2k^2K'(k)]}{(2-k^2)(1-2k^2)E'(k)^2+k^2(1+k^2)K'(k)E'(k)-k^4K'(k)^2}$$

$$\omega_r'=-\frac{(1+k^2)^{3/2}[2(1-k^2+k^4)E'(k)-k^2(1+k^2)K'(k)]}{2k[(2-k^2)(1-2k^2)E'(k)^2+k^2(1+k^2)K'(k)E'(k)-k^4K'(k)^2]}$$

ϵ infinitesimally small quantity

$$\gamma=\frac{x-B^2z\sigma}{\sqrt{1-B^2\sigma^2}\sqrt{x^2-B^2(y^2+z^2)}}$$

γ_0 expression for γ indicated at $y=0$, $\dfrac{1-B^2\sigma\theta}{\sqrt{1-B^2\sigma^2}\sqrt{1-B^2\theta^2}}$

ψ,ν variables used for integrating purposes

Y side force

N yawing moment

L' rolling moment

C_Y side-force coefficient, Y/qS

C_n yawing-moment coefficient, N/qSb

C_l rolling-moment coefficient, L'/qSb

$$C_{Y_\beta}=\left(\frac{\partial C_Y}{\partial \beta}\right)_{\beta\to 0}$$

$$C_{n_\beta}=\left(\frac{\partial C_n}{\partial \beta}\right)_{\beta\to 0}$$

$$C_{l_\beta}=\left(\frac{\partial C_l}{\partial \beta}\right)_{\beta\to 0}$$

$$C_{Y_p}=\left(\frac{\partial C_Y}{\partial \frac{pb}{V}}\right)_{p\to 0}$$

$$C_{n_p}=\left(\frac{\partial C_n}{\partial \frac{pb}{V}}\right)_{p\to 0}$$

$$C_{l_p}=\left(\frac{\partial C_l}{\partial \frac{pb}{V}}\right)_{p\to 0}$$

$$C_{Y_r}=\left(\frac{\partial C_Y}{\partial \frac{rb}{V}}\right)_{r\to 0}$$

$$C_{n_r}=\left(\frac{\partial C_n}{\partial \frac{rb}{V}}\right)_{r\to 0}$$

$$C_{l_r}=\left(\frac{\partial C_l}{\partial \frac{rb}{V}}\right)_{r\to 0}$$

$$C_{Y_{\dot\beta}}=\left(\frac{\partial C_Y}{\partial \frac{\dot\beta b}{V}}\right)_{\dot\beta\to 0}$$

$$C_{n_\beta}=\left(\frac{\partial C_n}{\partial \frac{\dot{\beta}b}{V}}\right)_{\beta\to 0}$$

$$C_{l_\beta}=\left(\frac{\partial C_l}{\partial \frac{\dot{\beta}b}{V}}\right)_{\dot{\beta}\to 0}$$

Subscripts:

p refers to rolling condition

r refers to yawing condition

$r=1$ refers to unit-yawing condition

β refers to sideslip condition

$\beta=1$ refers to unit-sideslip condition

$\dot{\beta}$ refers to constant-lateral-acceleration condition

w based on wing dimensions

1,2   components used for $\dot{\beta}$ derivatives

Abbreviations:

L. E.   leading edge

T. E.   trailing edge

All angles are measured in radians.

ANALYSIS

SCOPE

The vertical-tail plan forms considered herein are shown in figure 1. The leading edge has arbitrary sweepback and the trailing edge may be either sweptback or sweptforward. The permissible ranges of sweep, aspect ratio, and taper ratio for the supersonic-leading-edge configurations are determined by the conditions (indicated in fig. 1) that both the leading edges and trailing edges remain supersonic and that the Mach line emanating from the leading edge of the root chord does not intersect the tip chord. Also, the tip chord must be parallel to the root chord. For the subsonic leading-edge configurations, only the case of zero taper ratio is considered and the restriction to supersonic trailing edge is imposed.

Expressions based on linearized supersonic-flow theory are obtained for the perturbation velocity potentials and pressure distributions due to steady rolling, steady yawing, and constant lateral acceleration. For purposes of completeness, analogous results for constant sideslip motion obtainable, in general, from references 9 and 10 are included. The expressions, which are derived for the condition of zero geometric angle of attack and which are valid for low rates of angular velocities, small sidelip angles, and small angle-of-sideslip variation with time, are tabulated so that they may be utilized conveniently in the calculation of load distributions and the corresponding forces and moments.

Two important members of the family of vertical-tail plan forms are considered in detail. These are the rectangular tail and the triangular tail with an unswept trailing edge, that is, the half-delta tail. For these tails, closed-form expressions are derived for the side force, yawing moment, and rolling moment due to each motion. The resulting formulas are expressed in the form of stability derivatives and are tabulated; simple charts are presented which permit rapid estimation of the 12 stability derivatives for given values of aspect ratio and Mach number. Tabulation

of the derivatives for subsonic-edge triangular tails with trailing-edge sweep are also presented.

Three systems of body axes are employed in the present report. For plan-form integrations and in the derivation and presentation of velocity potentials and pressures, the conventional analysis system shown in figure 2 (a) is utilized. In order to maintain the usual stability system of positive forces and moments, the axes systems shown in figures 2 (b) and 2 (c) are used in formulating the stability derivatives. A table of transformation formulas is provided which enables the stability derivatives, presented herein with reference to a center of gravity (origin) located at the leading edge of the root chord (fig. 2(b)), to be obtained with reference to an arbitrary center-of-gravity location (fig. 2 (c)).

BASIC CONSIDERATIONS

The calculation of forces acting on the vertical tail essentially requires a knowledge of the distribution of the pressure difference between the two sides of the tail surface. This pressure-difference distribution is expressible in terms of the perturbation-velocity-potential difference or "potential jump across the surface" $\Delta\varphi$ by means of the linearized relationship

$$\frac{\Delta P}{q}=\frac{2}{V^2}\left(V\frac{\partial}{\partial x}\Delta\varphi+\frac{\partial}{\partial t}\Delta\varphi\right) \tag{1}$$

Inasmuch as for the present investigation thin isolated tail surfaces are considered and thus no induced effects are present from any neighboring surface, the perturbation velocity potentials on the two sides of the tail are equal in magnitude but are of opposite sign. Equation (1) may then be rewritten in terms of the perturbation velocity potential φ as follows:

$$\frac{\Delta P}{q}=\frac{4}{V^2}\left(V\frac{\partial\varphi}{\partial x}+\frac{\partial\varphi}{\partial t}\right) \tag{2}$$

where φ is evaluated on the positive y-side of the tail surface.

The basic problem, then, is to find for each motion under consideration the perturbation-velocity-potential function φ for the various tail regional areas formed either by plan-form or plan-form and Mach line boundaries. (See, for example, the sketch given in table I.)

For time-independent motions, such as steady rolling, steady yawing, and constant sideslip, the potential functions are of course independent of time (i. e., the last term in eqs. (1) and (2) vanishes) and may be determined for the subsonic-leading-edge cases by the doublet-distribution method of references 14 and 15. The details of the method and its application are given in the appendixes. The supersonic-leading edge configurations are analyzed by the well-known source-distribution method utilizing the area-cancellation—Mach line reflection technique of reference 16. The mathematical details are not presented herein, because it is felt that previous papers dealing with wing problems (e. g., refs. 17 to 20) have applied the basic method in sufficient detail. The main difference to be noted is that the root chord of the isolated vertical tail is, in effect, another free subsonic edge similar to the tip chord and must be treated accordingly. Actually, tail regions I and III (refer to the sketch in table I) are not affected by the additional

tip, and wing results in these regions for constant angle of attack (ref. 20), steady rolling (ref. 20), and steady pitching (ref. 18) are applicable to constant sideslip, steady rolling, and steady yawing motions, respectively, for the vertical tail, provided appropriate changes in coordinates are introduced and the proper sign convention is maintained.

The time-dependent motion considered in the present report, that is, constant lateral acceleration, can be analyzed in a manner analogous to that used for a wing surface undergoing constant vertical acceleration (e. g., refs. 21 to 23). By following this procedure, the basic expressions for the perturbation velocity potential and pressure coefficient (evaluated at time $t=0$) may be derived as follows:

$$\varphi = -\dot{\beta}\left[\frac{M^2}{B^2}\varphi_{r=1} - \left(t - \frac{M^2 x}{B^2 V}\right)\varphi_{\beta=1}\right] \quad (3)$$

$$\frac{\Delta P}{q} = -\frac{\dot{\beta}}{B^2}\left[M^2\left(\frac{\Delta P}{q}\right)_{r=1} + \frac{M^2 x}{V}\left(\frac{\Delta P}{q}\right)_{\beta=1} + \frac{4}{V^2}\varphi_{\beta=1}\right] \quad (4)$$

Equations (3) and (4) may be deduced directly from equations (1) and (2) of reference 23, provided the corresponding tail motion is substituted for each wing motion and, further, that care is exercised in preserving the conventional system of positive forces and moments. The choice of time $t=0$ in equation (4) was made for purposes of convenience and simplicity, inasmuch as the pressure due to constant sideslip is eliminated, and thus only the increment in pressure due to time rate of change of sideslip, that is, $\dot{\beta}$, remains.

The right-hand sides of equations (3) and (4) are composed of terms involving steady or time-independent motions, in particular, the motions previously discussed in this section. Thus, once the potentials and pressures are determined for steady yawing and constant sideslip, corresponding expressions may be obtained for constant lateral acceleration by use of equations (3) and (4).

Derivations of the potentials and pressures for the various regions of the tail plan forms under consideration have been carried out for each motion by using the methods and techniques discussed. Tabulations of the potential and pressure-distribution functions are given in tables I and II for constant sideslip, in tables III and IV for steady rolling, in tables V and VI for steady yawing, and in tables VII and VIII for constant lateral acceleration.

The forces and moments acting on the vertical tail due to each motion may be obtained by plan-form integrations of the appropriate potential and pressure functions and may be given as follows (the center of gravity is assumed to be at the leading edge of the root section):

$$Y = q\int_{\text{Root}}^{\text{Tip}}\int_{\text{L. E.}}^{\text{T. E.}}\frac{\Delta P}{q}dx\,dz \quad (5)$$

$$N = -q\int_{\text{Root}}^{\text{Tip}}\int_{\text{L. E.}}^{\text{T. E.}}\frac{\Delta P}{q}x\,dx\,dz \quad (6)$$

$$L' = q\int_{\text{Root}}^{\text{Tip}}\int_{\text{L. E.}}^{\text{T. E.}}\frac{\Delta P}{q}z\,dx\,dz \quad (7)$$

For steady motions, $\frac{\Delta P}{q} = \frac{4}{V}\frac{\partial\varphi}{\partial x}$ and thus the first integration with respect to x in equations (5) and (7) yields φ; hence, equations (5) and (7), when applied to steady motions, reduce

to essentially a single integration involving the potential function.

The nondimensional force and moment coefficients and corresponding stability derivatives are directly obtainable from the definitions given in the list of symbols. For example,

$$C_{n_r} = \left(\frac{\partial C_n}{\partial\frac{rb}{V}}\right)_{r\to 0}$$

$$= \left[\frac{\partial}{\partial\frac{rb}{V}}\left(\frac{N}{qSb}\right)\right]_{r\to 0}$$

$$= \left[\frac{\partial}{\partial\frac{rb}{V}}\left(-\frac{1}{Sb}\int_{\text{Root}}^{\text{Tip}}\int_{\text{L. E.}}^{\text{T. E.}}\frac{\Delta P}{q}x\,dx\,dz\right)\right]_{r\to 0}$$

Inasmuch as the various pressure coefficients are linear with reference to their respective angular velocities, attitude, or acceleration (i. e., linear in p, r, β, or $\dot{\beta}$), the partial derivative in the preceding example may be replaced by $\frac{1}{rb/V}$ and the derivative C_{n_r} is then expressed as

$$C_{n_r} = -\frac{1}{Sb^2\frac{r}{V}}\int_{\text{Root}}^{\text{Tip}}\int_{\text{L. E.}}^{\text{T. E.}}\frac{\Delta P}{q}x\,dx\,dz \quad (8)$$

Corresponding expressions for the 11 other derivatives C_{Y_β}, C_{n_β}, C_{l_β}, C_{Y_r}, C_{l_r}, C_{Y_p}, C_{n_p}, C_{l_p}, $C_{Y_{\dot{\beta}}}$, $C_{n_{\dot{\beta}}}$, and $C_{l_{\dot{\beta}}}$ may be obtained in an analogous manner.

In the present report, the triangular vertical tail with unswept trailing edge (half-delta) and the rectangular vertical tail have been analyzed in detail. The results obtained upon performing the plan-form integrations and other mathematical operations indicated in the previous discussion are tabulated in table IX. Table X presents similar results for the subsonic-edge triangular tails with trailing-edge sweep. For convenience, a table of transformation formulas is presented (table XI) which enables the derived results for the stability derivatives (tables IX and X) to be expressed with respect to an arbitrary center-of-gravity location.

Values of the elliptic-function parameters appearing in the subsonic-edge formulas are presented graphically in figure 3.

COMPUTATIONAL RESULTS AND DISCUSSION

The formulas for the stability derivatives given in tables IX and X are seen to be functions of the tail-aspect ratio A and the Mach number parameter $B=\sqrt{M^2-1}$. Use of the combined parameter AB for the abscissa variable and appropriate choice of derivative parameters for the ordinates allow the analytical results for most of the stability derivatives to be expressed graphically by means of a single simple curve; the stability derivatives due to $\dot{\beta}$-motion require two curves. Figures 4 to 9 present the results for the half-delta tail and figures 10 to 14 present the analogous results for the rectangular tail. The lower limit $AB=1$ for the rectangular vertical tail corresponds to the condition where the Mach line from the leading edge of the root chord intersects the trailing edge of the tip chord. Values of the derivatives for the situation where the Mach line from the leading edge of the root chord intersects the tip chord, that is, values of $AB<1$, cannot, in general, be obtained easily because of the

fact that the calculation involves the consideration of interacting external flow fields. The lower limit $AB=1$ in this case is not very restrictive except for very low aspect ratios at low supersonic Mach numbers.

In considering the curves given in figures 4 to 14, the following facts should be kept in mind: (a) The results are for a completely isolated vertical tail, (b) the center-of-gravity location is assumed to be at the tail apex, and (c) parameters used for nondimensionalizing purposes are the area and span of the vertical tail. For other center-of-gravity locations, analogous curves may be drawn by use of the presented data and the axes-transformation formulas given in table XI.

Thus far, only the isolated vertical tail has been considered, that is, the zero-end-plate solution. For comparison purposes, results for several of the derivatives based on a complete-end-plate analysis have been obtained and are presented in figures 15 and 16. The comparisons are shown for the side-force and yawing-moment derivatives due to constant sideslip, steady yawing, and constant lateral acceleration. The complete-end-plate results for these tail derivatives are obtainable from stability derivatives previously reported for symmetrical wings (refs. 18, 20, 23, and 24), provided modifications are introduced to account for (a) changes in nondimensionalizing parameters, (b) correspondence of wing and vertical-tail motions, and (c) preservation of sign convention for positive sense of motion, moments, and so forth. The transformations of symmetrical-wing derivatives into complete-end-plate derivatives for vertical tails having the same plan-form geometry as the half-wing may be summarized as follows:

$C_{Y_\beta} = -1 \times$ (Expression for C_{L_α} with wing aspect ratio replaced by $2A$)

$C_{n_\beta} = -\dfrac{4}{3A} \dfrac{1+\lambda+\lambda^2}{(1+\lambda)^2} \times$ (Expression for C_{m_α} with wing aspect ratio replaced by $2A$)

$C_{Y_r} = \dfrac{2}{3A} \dfrac{1+\lambda+\lambda^2}{(1+\lambda)^2} \times$ (Expression for C_{L_q} with wing aspect ratio replaced by $2A$)

$C_{n_r} = \dfrac{8}{9A^2} \dfrac{(1+\lambda+\lambda^2)^2}{(1+\lambda)^4} \times$ (Expression for C_{m_q} with wing aspect ratio replaced by $2A$)

$C_{Y_{\dot\beta}} = -\dfrac{2}{3A} \dfrac{1+\lambda+\lambda^2}{(1+\lambda)^2} \times$ (Expression for $C_{L_{\dot\alpha}}$ with wing aspect ratio replaced by $2A$)

$C_{n_{\dot\beta}} = -\dfrac{8}{9A^2} \dfrac{(1+\lambda+\lambda^2)^2}{(1+\lambda)^4} \times$ (Expression for $C_{m_{\dot\alpha}}$ with wing aspect ratio replaced by $2A$)

where C_{L_α}, C_{m_α}, C_{L_q}, C_{m_q}, $C_{L_{\dot\alpha}}$, and $C_{m_{\dot\alpha}}$ are conventionally defined wing derivatives (see, for example, ref. 23). Figures 15 and 16 indicate that for a given aspect ratio the effect of an end plate decreases with increasing Mach number and that for a given Mach number the effect of an end plate decreases with increasing aspect ratio. Although these conclusions apply specifically to those derivatives presented, it is felt that similar evidence would be found for the other derivatives as well. The percentage differences between zero- and complete-end-plate results vary of course with center-of-gravity location, as well as with Mach number and

aspect ratio, but in general are not too large for the side-force and yawing-moment derivatives considered except at the lower values of AB.

The stability derivatives as presented herein have been made nondimensional with respect to vertical-tail parameters such as tail span b, tail area S, and the angles pb/V, rb/V, and $\dot\beta b/V$. The magnitudes of the derivatives may, therefore, appear to be quite large with respect to the expected tail contributions to the derivatives for a complete airplane. The following factors should be used in converting the presented analytical and numerical results to corresponding derivatives (denoted in the following relationships by subscript w) based on wing area S_w, wing span b_w, and angles $pb_w/2V$, $rb_w/2V$, and $\dot\beta b_w/2V$:

$$\left(C_{Y_\beta}\right)_w = \frac{S}{S_w} C_{Y_\beta}$$

$$\left(C_{n_\beta}\right)_w, \left(C_{l_\beta}\right)_w = \frac{S}{S_w}\frac{b}{b_w}\left(C_{n_\beta}, C_{l_\beta}\right)$$

$$\left(C_{Y_p}\right)_w, \left(C_{Y_r}\right)_w, \left(C_{Y_{\dot\beta}}\right)_w = 2\frac{S}{S_w}\frac{b}{b_w}\left(C_{Y_p}, C_{Y_r}, C_{Y_{\dot\beta}}\right)$$

$$\left(C_{n_p}\right)_w, \left(C_{l_p}\right)_w, \left(C_{n_r}\right)_w, \left(C_{l_r}\right)_w, \left(C_{n_{\dot\beta}}\right)_w, \left(C_{l_{\dot\beta}}\right)_w$$

$$= 2\frac{S}{S_w}\left(\frac{b}{b_w}\right)^2\left(C_{n_p}, C_{l_p}, C_{n_r}, C_{l_r}, C_{n_{\dot\beta}}, C_{l_{\dot\beta}}\right)$$

CONCLUDING REMARKS

Velocity potentials, pressure distributions, and stability derivatives have been derived by use of supersonic linearized theory for families of thin isolated vertical tails performing steady rolling, steady yawing, and constant-lateral-acceleration motions. Vertical-tail families (half-delta and rectangular plan forms) are considered for a broad Mach number range. Also considered are the vertical tail with arbitrary sweepback and taper ratio at Mach numbers for which both the leading edge and trailing edge of the tail are supersonic and the triangular vertical tail with a subsonic leading edge and a supersonic trailing edge. For purposes of completeness, analogous expressions and derivatives for sideslip motion obtained primarily from other sources are included.

The effects of a complete end plate on several of the side-force and yawing-moment derivatives have been considered, and it appears that only for relatively small values of the aspect-ratio—Mach number parameter $A\sqrt{M^2-1}$ do the complete-end-plate and zero-end-plate values differ significantly enough to warrant further study of finite-end-plate corrections.

An additional point of interest pertinent to the present investigation is that the results obtained for the yawing-moment derivatives due to steady yawing and constant lateral acceleration C_{n_r} and $C_{n_{\dot\beta}}$ may be used to approximate the aerodynamic damping of the lateral oscillation in yaw to the first order in frequency. This approximation to the lateral damping is given by the expression $C_{n_r}-C_{n_{\dot\beta}}$ and can be rapidly calculated from the curves and formulas given herein.

LANGLEY AERONAUTICAL LABORATORY,
  NATIONAL ADVISORY COMMITTEE FOR AERONAUTICS,
  LANGLEY FIELD, VA., *March 5, 1956*.

APPENDIX A

DETERMINATION OF PRESSURE-DISTRIBUTION EXPRESSIONS FOR A SUBSONIC-EDGE TAIL UNDERGOING YAWING AND ROLLING MOTIONS

A method for solving supersonic-flow boundary-value problems governed by the classical, linearized, partial-differential equation

$$B^2 \frac{\partial^2 \varphi}{\partial x^2} - \frac{\partial^2 \varphi}{\partial y^2} - \frac{\partial^2 \varphi}{\partial z^2} = 0 \qquad (A1)$$

has been developed in reference 14 and an application to rolling and pitching triangular wings is given in reference 15. This method allows the prediction of the disturbance-potential function φ, and hence the pressure distribution, for planar lifting surfaces. The analysis given in reference 15 is briefly summarized herein and is applied to the determination of the pressure distributions on a triangular-vertical-tail surface (fig. 2) performing rolling and yawing motions. (Yawing in the xz-plane is analogous to pitching in the xy-plane.)

DETERMINATION OF THE FORM OF THE VELOCITY POTENTIAL

As is well-known, the potentials of both the supersonic source and the supersonic doublet and their distributions represent solutions of equation (A1). For the determination of the potentials and pressure distributions of lifting surfaces with subsonic leading edges, a distribution of doublets that uniquely satisfies the prescribed boundary conditions is required. The boundary conditions on the vertical tail for the motions to be considered herein are as follows:
On the rolling vertical tail,

$$v = pz = xp\frac{z}{x} = xp\theta \qquad (A2)$$

and on the yawing vertical tail,

$$v = -rx \qquad (A3)$$

In addition, the following relations must be valid on the surfaces of the tail:
For the rolling motion,

$$\frac{\partial \left(\frac{v}{x}\right)_p}{\partial \theta} = p \qquad (A4)$$

$$\frac{\partial^2 \left(\frac{v}{x}\right)_p}{\partial \theta^2} = 0 \qquad (A5)$$

and for the yawing motion,

$$\frac{\partial \left(\frac{v}{x}\right)_r}{\partial \theta} = 0 \qquad (A6)$$

$$\frac{\partial^2 \left(\frac{v}{x}\right)_r}{\partial \theta^2} = 0 \qquad (A7)$$

It is also necessary that the pressure along the streamwise edge be zero.

The potential in space produced by a distribution of doublets, for example, in the xz-plane, with the doublet axes normal to the plane is

$$\varphi_D(x, y, z) = \frac{\partial}{\partial y} \iint_S \frac{-A(\xi, \zeta) d\xi \, d\zeta}{\sqrt{(x-\xi)^2 - B^2(z-\zeta)^2 - B^2 y^2}} \qquad (A8)$$

where the area S is the region of the xz-plane intercepted by the forecone from the field point (x, y, z).
The potential on the surface carrying the doublet distribution is given by

$$\varphi_D(x,z)_{y=\pm 0} = \lim_{y \to \pm 0} \left[\frac{\partial}{\partial y} \iint_S \frac{-A(\xi, \zeta) d\xi \, d\zeta}{\sqrt{(x-\xi)^2 - B^2(z-\zeta)^2 - B^2 y^2}} \right]$$

As stated in reference 15, this surface potential is directly proportional to the doublet-strength function $A(x,z)$; that is,

$$\varphi_D(x,z)_{y=\pm 0} = \pm \pi A(x,z) \qquad (A9)$$

The surface-pressure velocity $u(x,z)$ then becomes

$$u(x,z)_{y=\pm 0} = \frac{\partial \varphi_D(x,z)_{y=\pm 0}}{\partial x} = \pm \pi \frac{\partial A(x,z)}{\partial x} \qquad (A10)$$

and the linearized pressure coefficient

$$\frac{\Delta P}{q} = \frac{4u(x,z)_{y=+0}}{V} \qquad (A11)$$

may be written as

$$\frac{\Delta P}{q} = \frac{4\pi}{V} \frac{\partial A(x,z)}{\partial x} \qquad (A12)$$

The problem to be considered in this appendix is one in which the sidewash on the surface is prescribed (see eqs. (A2) and (A3)) and the surface velocity potential has to be determined. The doublet-strength function $A(x,z)$ then is an unknown and the determination of this quantity requires in general the solution of an integral equation. In some cases the general form of the surface-potential function $A(x,z)$ is known or can be obtained by inverting an integral equation. The problem then resolves simply into an evaluation of the arbitrary constants of the general solution by making use of the prescribed boundary conditions.

Brown and Adams in their analysis of rolling and pitching triangular wings with subsonic leading edges (ref. 15) were able to determine the function $A(x,z)$ by utilizing the concept that the conical properties of the produced flow gave rise to potentials and pressures in the crossflow planes that were similar in form to the potentials and pressures acting on flat finite segments in a two-dimensional flow; these segments correspond to a section of the wing in any crossflow plane. This remarkable connection between linearized supersonic

conical flow and incompressible two-dimensional flow is discussed by Busemann in reference 25.

A more general and rigorous approach to obtain the doublet-strength function may be formulated from an analysis presented in a later paper by Lomax and Heaslet (ref. 26) dealing also with conical and the so-called quasi-conical problems. In this analysis a general surface-pressure-coefficient expression has been determined for planar lifting surfaces with prescribed boundary conditions of the form

$$v \sim x^\kappa g\left(\frac{z}{x}\right) \tag{A13}$$

This expression is

$$\frac{\Delta P}{q} = \left(\frac{x}{B}\right)^\kappa \sum_{i=0}^{\kappa+1} \frac{b_i \theta^i}{\sqrt{(m-\theta)(\theta-m_1)}} \tag{A14}$$

where b_i are constants, $\theta = \frac{z}{x}$, κ is determined by the boundary-condition equation (eq. (A13)), and m and m_1 are the tangents of the apex angles of the two panels of the lifting surface. When $m_1 = m$, the lifting surface is symmetrical about the common root chord of the two panels, and when $m_1 \neq m$, the lifting surface is asymmetrical about this chord. From equations (A12), (A14), and (A9) the form of $A(x,z)$ or, synonymously, the form of the surface potential may be obtained by a simple integration. It should be mentioned at this point that reference 26 presents a method for deriving the arbitrary constants b_i in the pressure coefficient (eq. (A14)). This method is related to that of reference 15 which concerns itself with obtaining the arbitrary constants in the velocity potential.

By application of equation (A14) to the boundary problem of the triangular vertical tail ($m_1 = 0$) and by noting from the prescribed boundary conditions (see eqs. (A2) and (A3)) that $\kappa = 1$, the pressure coefficient for both the yawing and rolling motions is

$$\frac{\Delta P}{q} = \frac{x}{B} \frac{b_0 + b_1 \theta + b_2 \theta^2}{\sqrt{(m-\theta)\theta}} \tag{A15}$$

The constant b_0 in this expression must be set equal to zero in order to satisfy the condition that along the streamwise edge the pressure must be zero.

The velocity potential on the vertical-tail surface is easily obtainable from the pressure expression by the formula

$$\varphi = \frac{V}{4} \int_{L.E.}^x \frac{\Delta P}{q} d\xi$$

and has been found to be

$$\varphi = \pi x^2 f\left(\frac{z}{x}\right) \tag{A16}$$

where

$$f\left(\frac{z}{x}\right) = f(\theta) = (\tau\theta + \omega m)\sqrt{\theta(m-\theta)} \tag{A17}$$

The arbitrary constants τ and ω in the so-called distribution function $f(\theta)$ are, in terms of b_1 and b_2,

$$\tau = \frac{V}{2\pi B}\left(\frac{2b_1}{3m^2} + \frac{b_2}{m}\right)$$

$$\omega = \frac{V}{2\pi B}\frac{b_1}{3m^2}$$

By relating equation (A16) to equation (A9), the doublet-strength function $A(x,z)$ is seen to be

$$A(x,z) = x^2 f\left(\frac{z}{x}\right) \tag{A18}$$

A comparison of the potential given by equations (A16) and (A17) and the potential obtained for the slender, rolling, vertical tail reported in reference 5 shows, as expected, that both are of the same form.

EVALUATION OF THE CONSTANTS τ AND ω

The constants τ and ω in the expressions for the velocity potential given by equations (A16) and (A17) are still to be determined. As indicated previously, the expression for the pressure coefficient, and hence the velocity potential, can be determined completely through an application of the procedures developed in reference 26; however, many of the integrations and integrating procedures required in the method in reference 15 were already known to the junior author at the inception of this project and, for this reason, the analysis herein to determine the constants τ and ω closely parallels the procedures discussed in reference 15.

The determination of the constants τ and ω depends upon satisfying the boundary conditions associated with the vertical tail for the rolling and yawing motions. These boundary conditions are given by equations (A2) to (A7). The needed expressions for the prescribed velocities and their derivatives with respect to θ in terms of the distribution function $f(\sigma)$ are derived in appendix B.

For the rolling motion the constants τ and ω may be obtained by replacing $f(\sigma)$ by its equivalent (eq. (A17)) in the equations given in appendix B for v/x and $\frac{\partial(v/x)}{\partial\theta}$ and then applying the boundary conditions given by equations (A2) and (A4). When the integrations have been performed, the resulting equations may be solved simultaneously for τ_p and ω_p. The yawing constants are obtained in a like manner with equations (A3) and (A6) replacing equations (A2) and (A4), respectively.

In the calculation of the quantities v/x and $\frac{\partial(v/x)}{\partial\theta}$, any value of θ may be considered. It is advantageous for integration purposes to let this value of θ be zero. However, since one of the limits of integration is zero and since in several of the integrands a singular point exists at $\theta = \sigma = 0$, the integrations in which these singularities occur must be performed for θ arbitrary before θ can be set equal to zero.

Substituting equation (A17) into equation (B4) gives, for θ equal to zero,

$$\frac{v}{x}=\frac{1}{B}\int_0^{Bm}\left[\frac{-3(\tau B\sigma+\omega Bm)\sqrt{B\sigma(Bm-B\sigma)}\tanh^{-1}\sqrt{1-B^2\sigma^2}}{(1-B^2\sigma^2)^{5/2}}+\frac{2(\tau B\sigma+\omega Bm)\sqrt{B\sigma(Bm-B\sigma)}}{(1-B^2\sigma^2)^2}\right]d(B\sigma)+$$

$$\lim_{\theta\to0}\left\{\lim_{\epsilon\to0}\left[\frac{1}{B}\int_0^{B(\theta-\epsilon)}\frac{(\tau B\sigma+\omega Bm)\sqrt{B\sigma(Bm-B\sigma)}(1-B^2\sigma\theta)^2\sqrt{1-B^2\theta^2}}{(1-B^2\sigma^2)^2(B\sigma-B\theta)^2}d(B\sigma)+\right.\right.$$

$$\left.\left.\frac{1}{B}\int_{B(\theta+\epsilon)}^{Bm}\frac{(\tau B\sigma+\omega Bm)\sqrt{B\sigma(Bm-B\sigma)}(1-B^2\sigma\theta)^2\sqrt{1-B^2\theta^2}}{(1-B^2\sigma^2)^2(B\sigma-B\theta)^2}d(B\sigma)-\frac{2(\tau B\theta+\omega Bm)\sqrt{B\theta(Bm-B\theta)}\sqrt{1-B^2\theta^2}}{B^2\epsilon}\right]\right\}\qquad\text{(A19)}$$

Carrying out the integrations in equation (A19) yields

$$\frac{v}{x}=\frac{-\pi}{B\sqrt{1+k^2}(1-k^2)^2}\{K'(k)[2k^3\tau+\bar{\omega}k^2(1+k^2)]-E'(k)[\tau k(1+k^2)-\bar{\omega}(1-4k^2+k^4)]\}\qquad\text{(A20)}$$

where

$$k=\frac{1-\sqrt{1-B^2m^2}}{Bm}\qquad\text{(A21)}$$

and

$$\bar{\omega}=\omega Bm=\omega\frac{2k}{1+k^2}$$

These integrations were accomplished with the aid of the tables in references 27 and 28 and are discussed in appendix C. Substituting the distribution function into equation (B5) results in, for θ approaching zero,

$$\frac{\partial(v/x)}{\partial\theta}=\int_0^{Bm}\left[\frac{3B\sigma(\tau B\sigma+\omega Bm)\sqrt{B\sigma(Bm-B\sigma)}\tanh^{-1}\sqrt{1-B^2\sigma^2}}{(1-B^2\sigma^2)^{5/2}}-\frac{3B\sigma(\tau B\sigma+\omega Bm)\sqrt{B\sigma(Bm-B\sigma)}}{(1-B^2\sigma^2)^2}\right]d(B\sigma)+$$

$$\lim_{\theta\to0}\left(\lim_{\epsilon\to0}\left\{\int_0^{B(\theta-\epsilon)}\left[\frac{B\theta(\tau B\sigma+\omega Bm)\sqrt{B\sigma(Bm-B\sigma)}}{\sqrt{1-B^2\theta^2}(B\sigma-B\theta)^2}-\frac{(\tau B\sigma+\omega Bm)\sqrt{B\sigma(Bm-B\sigma)}}{\sqrt{1-B^2\theta^2}(1-B^2\sigma^2)(B\sigma-B\theta)}+\right.\right.\right.$$

$$\left.\frac{2(\tau B\sigma+\omega Bm)\sqrt{B\sigma(Bm-B\sigma)}\sqrt{1-B^2\theta^2}}{(B\sigma-B\theta)^3}\right]d(B\sigma)+\int_{B(\theta+\epsilon)}^{Bm}\left[\frac{B\theta(\tau B\sigma+\omega Bm)\sqrt{B\sigma(Bm-B\sigma)}}{\sqrt{1-B^2\theta^2}(B\sigma-B\theta)^2}-\right.$$

$$\frac{(\tau B\sigma+\omega Bm)\sqrt{B\sigma(Bm-B\sigma)}}{\sqrt{1-B^2\theta^2}(1-B^2\sigma^2)(B\sigma-B\theta)}+\frac{2(\tau B\sigma+\omega Bm)\sqrt{B\sigma(Bm-B\sigma)}\sqrt{1-B^2\theta^2}}{(B\sigma-B\theta)^3}\bigg]d(B\sigma)-$$

$$\left.\left.\frac{2B\theta(\tau B\theta+\omega Bm)\sqrt{B\theta(B\theta-Bm)}}{B\epsilon\sqrt{1-B^2\theta^2}}-\frac{2[-4B^2\theta^2\tau+B\theta Bm(3\tau-2\omega)+\omega B^2m^2]\sqrt{1-B^2\theta^2}}{B\epsilon\sqrt{B\theta(B\theta-Bm)}}\right\}\right)\qquad\text{(A22)}$$

By performing the integrations in equation (A22), the following expression is obtained:

$$\frac{\partial(v/x)}{\partial\theta}=\frac{\pi}{\sqrt{1+k^2}(1-k^2)^2}[k^2K'(k)(\tau+\tau k^2+2\bar{\omega}k)+E'(k)(2\tau k^2-2\tau-\bar{\omega}k-2\tau k^4-\bar{\omega}k^3)]\qquad\text{(A23)}$$

Consider the rolling case for which $\tau=\tau_p$ and $\omega=\omega_p$. Also from equations (A2) and (A4), for $\theta=0$, $v/x=0$ and $\dfrac{\partial(v/x)}{\partial\theta}=p$.

Solving equations (A20) and (A23) for τ_p and ω_p, with $\bar{\omega}=Bm\omega_p=\dfrac{2k}{1+k^2}\omega_p$, gives

$$\tau_p=\frac{-p\sqrt{1+k^2}[k^2(1+k^2)K'(k)+(1-4k^2+k^4)E'(k)]}{\pi[-k^4K'(k)^2+k^2(1+k^2)K'(k)E'(k)+(2-k^2)(1-2k^2)E'(k)^2]}\qquad\text{(A24)}$$

$$\omega_p=\frac{p(1+k^2)^{3/2}[2k^2K'(k)-(1+k^2)E'(k)]}{2\pi[-k^4K'(k)^2+k^2(1+k^2)K'(k)E'(k)+(2-k^2)(1-2k^2)E'(k)^2]}\qquad\text{(A25)}$$

For the yawing case $\tau = \tau_r$, $\bar{\omega} = \dfrac{2k}{1+k^2}\,\omega_r$, and, from equations (A3) and (A6) $\dfrac{v}{x} = -r$ and $\dfrac{\partial(v/x)_r}{\partial\theta} = 0$, respectively. Solving equations (A20) and (A23) simultaneously after making these substitutions yields

$$\tau_r = \frac{Brk\sqrt{1+k^2}\,[2k^2K'(k) - (1+k^2)E'(k)]}{\pi[-k^4K'(k)^2 + k^2(1+k^2)K'(k)E'(k) + (2-k^2)(1-2k^2)E'(k)^2]} \tag{A26}$$

$$\omega_r = \frac{-Br(1+k^2)^{3/2}[k^2(1+k^2)K'(k) - 2(1-k^2+k^4)E'(k)]}{2\pi k[-k^4K'(k)^2 + k^2(1+k^2)K'(k)E'(k) + (2-k^2)(1-2k^2)E'(k)^2]} \tag{A27}$$

It is convenient for plotting purposes and in expressing the aerodynamic coefficients to make the following definitions:

$$\left.\begin{aligned}
\tau_r &= \tau_r{}' \frac{Br}{\pi} \\[2mm]
\omega_r &= \omega_r{}' \frac{Br}{\pi} \\[2mm]
\tau_p &= \tau_p{}' \frac{p}{\pi} \\[2mm]
\omega_p &= \omega_p{}' \frac{p}{\pi}
\end{aligned}\right\} \tag{A28}$$

so that $\tau_r{}'$, $\omega_r{}'$, $\tau_p{}'$, and $\omega_p{}'$ are functions of the Bm only. The variations of these four parameters with Bm are shown in figure 3.

The velocity potentials for the rolling and yawing motions, completely defined by equations (A16) and (A17) and the constants given in equations (A21), (A24), (A25), (A26), (A27), and (A28), may now be written as

and

$$\varphi_p = px^2(\tau_p{}'\theta + \omega_p{}'m)\sqrt{\theta(m-\theta)} \tag{A29}$$

$$\varphi_r = Brx^2(\tau_r{}'\theta + \omega_r{}'m)\sqrt{\theta(m-\theta)} \tag{A30}$$

The pressure coefficients for the rolling and yawing motions found from equations (A29), (A30), (A10), and (A11) are

and

$$\left(\frac{\Delta P}{q}\right)_p = \frac{2p}{V}\,\frac{\tau_p{}'mz^2 + 3m^2\omega_p{}'xz - 2m\omega_r{}'z^2}{\sqrt{z(mx-z)}} \tag{A31}$$

$$\left(\frac{\Delta P}{q}\right)_r = \frac{2Br}{V}\,\frac{\tau_r{}'mz^2 + 3m^2\omega_r{}'xz - 2m\omega_r{}'z^2}{\sqrt{z(mx-z)}} \tag{A32}$$

APPENDIX B

DEVELOPMENT OF EQUATIONS RELATING THE v-VELOCITY TO THE DISTRIBUTION FUNCTION $f(\sigma)$ IN THE $y=0$ PLANE

Equation (A8) gives the expression for the velocity potential (everywhere in space) resulting from a distribution of doublets in the xz-plane with the strength of each doublet in this distribution being governed by the doublet-strength function $A(x,z)$. The derivative of this velocity potential with respect to any one of the coordinates x, y, or z will give the perturbation velocity in that direction. Of primary interest herein is the v-velocity or the y-derivative of this potential

$$v(x,y,z)=\frac{\partial\varphi_D(x,y,z)}{\partial y} \tag{B1}$$

for points on the xz-plane. Brown and Adams in reference 15 have constructed the velocity potential in space of a distribution of doublets by the following approach. First, by using equations (A8) and (A18), the potential of a line of doublets in the xz-plane at an angle $\tan^{-1}\sigma$ to the x-axis is determined. This potential is given by

$$\varphi_L=-\frac{B^2y(x-B^2\sigma z)}{(1-B^2\sigma^2)^{5/2}}\left(3\coth^{-1}\gamma-\frac{\gamma}{\gamma^2-1}\right)+\frac{2B^2y\sqrt{x^2-B^2(y^2+z^2)}}{(1-B^2\sigma^2)^2} \tag{B2}$$

where

$$\gamma=\frac{x-B^2\sigma z}{\sqrt{1-B^2\sigma^2}\sqrt{x^2-B^2(y^2+z^2)}}$$

The velocity potential of a distribution of line doublets (i. e., a surface distribution) in the xz-plane, on the vertical tail, with strengths governed by the distribution function $f(\sigma)$ may then be written as

$$\varphi=\int_0^m f(\sigma)\varphi_L d\sigma \tag{B3}$$

where $\tan^{-1}m$ is the apex angle of the vertical tail.

Substituting equation (B2) into equation (B3) and differentiating with respect to y yield the following equation for the v-velocity as $\beta y/x$ approaches zero (see ref. 15):

$$\frac{v}{x}=\lim_{\epsilon\to 0}\left\{\int_0^{B(\theta-\epsilon)}\left[\frac{Bf(\sigma)\sqrt{1-B^2\theta^2}(1-B^2\sigma\theta)^2}{(1-B^2\sigma^2)^2(B\sigma-B\theta)^2}-\frac{3Bf(\sigma)(1-B^2\sigma\theta)\coth^{-1}\gamma_0}{(1-B^2\sigma^2)^{5/2}}+\frac{2Bf(\sigma)\sqrt{1-B^2\theta^2}}{(1-B^2\sigma^2)^2}\right]d(B\sigma)+\right.$$

$$\left.\int_{B(\theta+\epsilon)}^{Bm}\left[\frac{Bf(\sigma)\sqrt{1-B^2\theta^2}(1-B^2\sigma\theta)^2}{(1-B^2\sigma^2)^2(B\sigma-B\theta)^2}-\frac{3Bf(\sigma)(1-B^2\sigma\theta)\coth^{-1}\gamma_0}{(1-B^2\sigma^2)^{5/2}}+\frac{2Bf(\sigma)\sqrt{1-B^2\theta^2}}{(1-B^2\sigma^2)^2}\right]d(B\sigma)-\frac{2f(\theta)\sqrt{1-B^2\theta^2}}{\epsilon}\right\} \tag{B4}$$

The singularity which occurs in the $\dfrac{\gamma}{\gamma^2-1}$ term of equation (B2) when y is set equal to zero has been accounted for in equation (B4).

By taking the first and second derivatives of equation (B4) with respect to θ, two other useful relations are obtained. They are given in the appendix of reference 15 as

$$\frac{\partial(v/x)}{\partial\theta}=\lim_{\epsilon\to 0}\left\{\int_0^{B(\theta-\epsilon)}\left[\frac{3B^3\sigma f(\sigma)\coth^{-1}\gamma_0}{(1-B^2\sigma^2)^{5/2}}-\frac{B^2(3B\sigma+2B\theta+B\theta B^2\sigma^2)f(\sigma)}{\sqrt{1-B^2\theta^2}(1-B^2\sigma^2)^2}+\frac{B\theta B^2 f(\sigma)}{\sqrt{1-B^2\theta^2}(B\sigma-B\theta)^2}-\frac{B^2 f(\sigma)}{\sqrt{1-B^2\theta^2}(1-B^2\sigma^2)(B\sigma-B\theta)}+\right.\right.$$

$$\left.\frac{2B^2 f(\sigma)\sqrt{1-B^2\theta^2}}{(B\sigma-B\theta)^3}\right]d(B\sigma)+\int_{B(\theta+\epsilon)}^{Bm}\left[\frac{3B^3\sigma f(\sigma)\coth^{-1}\gamma_0}{(1-B^2\sigma^2)^{5/2}}-\frac{B^2(3B\sigma+2B\theta+B\theta B^2\sigma^2)f(\sigma)}{\sqrt{1-B^2\theta^2}(1-B^2\sigma^2)^2}+\frac{B\theta B^2 f(\sigma)}{\sqrt{1-B^2\theta^2}(B\sigma-B\theta)^2}-\right.$$

$$\left.\left.\frac{B^2 f(\sigma)}{\sqrt{1-B^2\theta^2}(1-B^2\sigma^2)(B\sigma-B\theta)}+\frac{2B^2 f(\sigma)\sqrt{1-B^2\theta^2}}{(B\sigma-B\theta)^3}\right]d(B\sigma)-\frac{2B^2\theta f(\theta)}{\epsilon\sqrt{1-B^2\theta^2}}-\frac{4\sqrt{1-B^2\theta^2}f'(\theta)}{\epsilon}\right\} \tag{B5}$$

and

$$\frac{\partial^2(v/x)}{\partial\theta^2}=\lim_{\epsilon\to 0}\left\{6\sqrt{1-B^2\theta^2}\int_0^{B(\theta-\epsilon)}\frac{B^3 f(\sigma)}{(B\sigma-B\theta)^4}d(B\sigma)+6\sqrt{1-B^2\theta^2}\int_{B(\theta+\epsilon)}^{Bm}\frac{B^3 f(\sigma)}{(B\sigma-B\theta)^4}d(B\sigma)-\sqrt{1-B^2\theta^2}\left[\frac{6f''(\theta)}{\epsilon}+\frac{4f(\theta)}{\epsilon^3}\right]\right\} \tag{B6}$$

The factor multiplying the $f''(\theta)$ term of the expression for $\dfrac{\partial^2(v/x)}{\partial\theta^2}$ as it appears in reference 15 is slightly in error and has been corrected in equation (B6). (The symbols $f'(\theta)$ and $f''(\theta)$ denote the first and second derivatives, respectively, with respect to θ.)

Considering equations (A5) and (A7), it is evident that equation (B6) must be zero for both the rolling and yawing cases. This equation has already been satisfied by $f(\theta)$ (eq. (A17)), since equation (B6) is in essence the integral equation which was inverted to obtain the general pressure expression from which $f(\theta)$ was derived (see ref. 26).

APPENDIX C

INTEGRATIONS TO OBTAIN v/x

The expression for v/x is, for θ approaching 0 (see eq. (A19)),

$$\frac{v}{x}=\frac{1}{B}\int_0^{B m}\left[\overset{\textstyle①}{\frac{-3(\tau B\sigma+\omega Bm)\sqrt{B\sigma(Bm-B\sigma)}\tanh^{-1}\sqrt{1-B^2\sigma^2}}{(1-B^2\sigma^2)^{5/2}}}+\right.$$

$$\left.\overset{\textstyle②}{\frac{2(\tau B\sigma+\omega Bm)\sqrt{B\sigma(Bm-B\sigma)}}{(1-B^2\sigma^2)^2}}\right]d(B\sigma)+$$

$$\lim_{\theta\to0}\left\{\lim_{\epsilon\to0}\left[\frac{1}{B}\int_0^{B(\theta-\epsilon)}\overset{\textstyle③a}{\frac{(\tau B\sigma+\omega Bm)\sqrt{B\sigma(Bm-B\sigma)}(1-B^2\sigma\theta)^2\sqrt{1-B^2\theta^2}}{(1-B^2\sigma^2)^2(B\sigma-B\theta)^2}}\,d(B\sigma)+\right.\right.$$

$$\int_{B(\theta+\epsilon)}^{B m}\overset{\textstyle③b}{\frac{(\tau B\sigma+\omega Bm)\sqrt{B\sigma(Bm-B\sigma)}(1-B^2\sigma\theta)^2\sqrt{1-B^2\theta^2}}{(1-B^2\sigma^2)^2(B\sigma-B\theta)^2}}\,d(B\sigma)-$$

$$\left.\left.\overset{\textstyle④}{\frac{2(\tau B\theta+\omega Bm)\sqrt{B\theta(Bm-B\theta)}\sqrt{1-B^2\theta^2}}{B^2\epsilon}}\right]\right\}\tag{C1}$$

This expression has been broken into parts as indicated by the circled numbers with the third part being broken into two additional parts ③a and ③b because of the singularity in the integrand. Since ② and ③ are elementary integrations similar to those found in most integral tables (see ref. 27), only ① will be dealt with in detail. Performing the integrations ② and ③ and combining the results yield

$$\frac{\sqrt{1-B^2\theta^2}}{B}\left\{\frac{2(\tau B\theta+\bar{\omega})\sqrt{B\theta(Bm-B\theta)}}{B\epsilon}-\frac{\pi[\tau(-7B\theta Bm-2+10B\theta-Bm)+\bar{\omega}(4-7Bm+4B\theta-B\theta Bm)]}{8\sqrt{1-Bm}(1-B\theta)}+\right.$$

$$\left.\frac{\pi[\tau(-2-10B\theta+Bm-7B\theta Bm)+\bar{\omega}(-4+4B\theta-7Bm+B\theta Bm)]}{8\sqrt{1+Bm}(1+B\theta)}\right\}\tag{C2}$$

where $\bar{\omega}=\omega Bm$. The first term of expression (C2) exactly cancels ④, so that the total of ②, ③, and ④ for $\theta\to0$ is

$$\frac{\pi}{8B}\left[\frac{\tau(2+Bm)-\bar{\omega}(4-7Bm)}{\sqrt{1-Bm}}+\frac{\tau(-2+Bm)-\bar{\omega}(4+7Bm)}{\sqrt{1+Bm}}\right]\tag{C3}$$

The following two integrals comprising ① remain to be evaluated:

$$\frac{-3}{B}\int_0^{B m}\frac{\tau B\sigma\sqrt{B\sigma(Bm-B\sigma)}\tanh^{-1}\sqrt{1-B^2\sigma^2}}{(1-B^2\sigma^2)^{5/2}}\,d(B\sigma)\tag{C4}$$

$$\frac{-3}{B}\int_0^{B m}\frac{\bar{\omega}\sqrt{B\sigma(Bm-B\sigma)}\tanh^{-1}\sqrt{1-B^2\sigma^2}}{(1-B^2\sigma^2)^{5/2}}\,d(B\sigma)\tag{C5}$$

It might be mentioned at this point that the integrands of expressions (C4) and (C5) are finite and continuous over the interval 0 to Bm and therefore must yield a finite quantity when integrated.

The integration of expression (C4) by parts gives

$$\left[\frac{-\tau\sqrt{B\sigma(Bm-B\sigma)}\tanh^{-1}\sqrt{1-B^2\sigma^2}}{B(1-B^2\sigma^2)^{3/2}}\right]_0^{B m}+\frac{\tau}{B}\left[\int_0^{B m}\frac{(Bm-2B\sigma)\tanh^{-1}\sqrt{1-B^2\sigma^2}}{2(1-B^2\sigma^2)^{3/2}\sqrt{B\sigma(Bm-B\sigma)}}\,d(B\sigma)-\int_0^{B m}\frac{\sqrt{B\sigma(Bm-B\sigma)}}{B\sigma(1-B^2\sigma^2)^2}\,d(B\sigma)\right]\tag{C6}$$

Integration of expression (C5) by parts gives

$$\left[\frac{-\bar{\omega}\sqrt{B\sigma(Bm-B\sigma)}\tanh^{-1}\sqrt{1-B^2\sigma^2}}{BB\sigma(1-B^2\sigma^2)^{3/2}}\right]_0^{B m}-\int_0^{B m}\frac{\bar{\omega}Bm\tanh^{-1}\sqrt{1-B^2\sigma^2}}{2BB\sigma(1-B^2\sigma^2)^{3/2}\sqrt{B\sigma(Bm-B\sigma)}}\,d(B\sigma)-\int_0^{B m}\frac{\bar{\omega}\sqrt{B\sigma(Bm-B\sigma)}}{BB^2\sigma^2(1-B^2\sigma^2)^2}\,d(B\sigma)\tag{C7}$$

Combining expressions (C6) and (C7) results in

$$① = \left[\frac{-(\tau B\sigma + \bar{\omega})\sqrt{B\sigma(Bm - B\sigma)}\,\tanh^{-1}\sqrt{1 - B^2\sigma^2}}{BB\sigma(1 - B^2\sigma^2)^{3/2}} \right]_0^{Bm} - \int_0^{Bm} \frac{(\tau B\sigma + \bar{\omega})\sqrt{B\sigma(Bm - B\sigma)}}{BB^2\sigma^2(1 - B^2\sigma^2)^2}\, d(B\sigma) +$$

$$\int_0^{Bm} \frac{[\tau B\sigma(Bm - 2B\sigma) - \bar{\omega}Bm]\,\tanh^{-1}\sqrt{1 - B^2\sigma^2}}{2BB\sigma(1 - B^2\sigma^2)^{3/2}\sqrt{B\sigma(Bm - B\sigma)}}\, d(B\sigma) \tag{C8}$$

The first term of equation (C8), when evaluated at the limits, is either zero or infinity. The integrand of ①, as was noted, is finite over the whole interval; therefore, infinities introduced as a result of parts integrations must, in the end, cancel themselves.

The second term of equation (C8) is an elementary integration which when evaluated (with infinities neglected) yields

$$\frac{\pi}{8B}\left(\frac{2\tau + 4\bar{\omega} - 3\tau Bm - 5\bar{\omega}Bm}{\sqrt{1 - Bm}} - \frac{-4\bar{\omega} - 5\bar{\omega}Bm + 2\tau + 3\tau Bm}{\sqrt{1 + Bm}} \right) \tag{C9}$$

It is now convenient in integrating the third term in equation (C8) to introduce the variable substitution

$$B\sigma = \frac{\psi + k}{1 + k\psi} \tag{C10}$$

so that Bm and k are related by

$$Bm = \frac{2k}{1 + k^2} \tag{C11}$$

The third term in equation (C8) when transformed by equation (C10) may be written in the form

$$\frac{-1}{B\sqrt{1 + k^2}(1 - k^2)} \sum_{i=1}^{7} I_i \tag{C12}$$

where

$$I_1 = \int_{-k}^{k} \frac{\tau(1 + k^4)\psi}{1 - \psi^2} F(\psi)\,d\psi$$

$$I_2 = -\int_{-k}^{k} k(\tau + \bar{\omega}k^3) F(\psi)\,d\psi$$

$$I_3 = \int_{-k}^{k} \frac{\tau k(1 + k^2) + 3\bar{\omega}k^2}{1 - \psi^2} F(\psi)\,d\psi$$

$$I_4 = \int_{-k}^{k} \frac{\bar{\omega}k^4(k^2 - 2)}{k^2 - \psi^2} F(\psi)\,d\psi$$

$$I_5 = \int_{-k}^{k} \frac{3\bar{\omega}k^3\psi}{k^2 - \psi^2} F(\psi)\,d\psi$$

$$I_6 = \int_{-k}^{k} \frac{\bar{\omega}k^2(1 - k^2)}{(1 - \psi^2)(k^2 - \psi^2)} F(\psi)\,d\psi$$

$$I_7 = -\int_{-k}^{k} \frac{\bar{\omega}k(1 - k^4\psi^2)\psi}{(1 - \psi^2)(k^2 - \psi^2)} F(\psi)\,d\psi$$

$$F(\psi) = \frac{\tanh^{-1}\left(\frac{\sqrt{1 - k^2}\sqrt{1 - \psi^2}}{1 + k\psi} \right)}{\sqrt{(1 - \psi^2)(k^2 - \psi^2)}}$$

The integrals I_1, I_5, and I_7 are elementary and may be determined by an integration by parts. If the multiplicative factor

before the summation sign in equation (C12) is neglected until all the components are totaled, these three components become

$$I_1+I_5+I_7=\frac{-\tau k(1+k^4)\pi}{1-k^2}-\frac{\bar{\omega}k^2(1+k^2)\pi}{1-k^2} \tag{C13}$$

Consider the integration required for I_2, that is,

$$\int_{-k}^{k}\frac{\tanh^{-1}\left[\frac{\sqrt{(1-k^2)(1-\psi^2)}}{1+k\psi}\right]}{\sqrt{(1-\psi^2)(k^2-\psi^2)}}d\psi \tag{C14}$$

Let $\psi=k\sin\theta$; then expression (C14) becomes

$$\int_{-\pi/2}^{\pi/2}\frac{\tanh^{-1}\left[\frac{\sqrt{(1-k^2)(1-k^2\sin^2\theta)}}{1+k^2\sin\theta}\right]}{\sqrt{1-k^2\sin^2\theta}}d\theta \tag{C15}$$

It can be shown that

$$\tanh^{-1}\left[\frac{\sqrt{(1-k^2)(1-k^2\sin^2\theta)}}{1+k^2\sin\theta}\right]=\tanh^{-1}\frac{\sqrt{1-k^2}}{\sqrt{1-k^2\sin^2\theta}}-\tanh^{-1}\frac{\sqrt{1-k^2}\sin\theta}{\sqrt{1-k^2\sin^2\theta}}\quad 0\leqq\theta\leqq\pi/2 \left.\begin{array}{c}\\\\\\\\\end{array}\right\}$$

$$=\tanh^{-1}\frac{\sqrt{1-k^2}}{\sqrt{1-k^2\sin^2\theta}}+\tanh^{-1}\frac{-\sqrt{1-k^2}\sin\theta}{\sqrt{1-k^2\sin^2\theta}}\quad 0\geqq\theta\geqq-\pi/2 \tag{C16}$$

This fact allows expression (C15) to be written as

$$\int_{-\pi/2}^{\pi/2}\frac{\tanh^{-1}\left(\frac{\sqrt{1-k^2}}{\sqrt{1-k^2\sin^2\theta}}\right)}{\sqrt{1-k^2\sin^2\theta}}d\theta-\int_0^{\pi/2}\frac{\tanh^{-1}\left(\frac{\sqrt{1-k^2}\sin\theta}{\sqrt{1-k^2\sin^2\theta}}\right)}{\sqrt{1-k^2\sin^2\theta}}d\theta+\int_{-\pi/2}^0\frac{\tanh^{-1}\left(\frac{-\sqrt{1-k^2}\sin\theta}{\sqrt{1-k^2\sin^2\theta}}\right)}{\sqrt{1-k^2\sin^2\theta}}d\theta \tag{C17}$$

The last two integrals of expression (C17) cancel each other and leave

$$2\int_0^{\pi/2}\frac{\tanh^{-1}\left(\frac{\sqrt{1-k^2}}{\sqrt{1-k^2\sin^2\theta}}\right)}{\sqrt{1-k^2\sin^2\theta}}d\theta \tag{C18}$$

After the inverse hyperbolic tangent is replaced by its logarithmic equivalent and the additional variable transformation

$$\sin^2\nu=\frac{1-k^2}{1-k^2\sin^2\theta} \tag{C19}$$

is introduced, expression (C18) becomes

$$\int_{\sin^{-1}\sqrt{1-k^2}}^{\pi/2}\left(\log_e\frac{1+\sin\nu}{1-\sin\nu}\right)\frac{d\nu}{\sqrt{\sin^2\nu-(1-k^2)}} \tag{C20}$$

It is now convenient to make the substitution

$$\delta=\sin^{-1}\sqrt{1-k^2}$$

Expression (C20) then becomes

$$\int_{\delta}^{\pi/2}\left(\log_e\frac{1+\sin\nu}{1-\sin\nu}\right)\frac{d\nu}{\sqrt{\sin^2\nu-\sin^2\delta}} \tag{C21}$$

which is exactly in the form of the fourth integration formula of table 335 in reference 28. This formula gives the value of expression (C21) as $\pi K'(k)$. The integration of I_2 may now be expressed as

$$I_2=-k(\tau+\bar{\omega}k^3)\pi K'(k) \tag{C22}$$

Using the same integrating procedure for I_3, I_4, and I_6 as just outlined for I_2 and the integration formulas in tables 335 and 336 of reference 28 leads to

$$I_3=\frac{[\tau k(1+k^2)+3\bar{\omega}k^2][1+K'(k)-E'(k)]\pi}{1-k^2}$$

$$I_4+I_6=\pi\bar{\omega}(1-k^2)k^2\Pi\left[-(1-k^2),\sqrt{1-k^2},\frac{\pi}{2}\right]-\bar{\omega}(1-k^2)k^2\pi K'(k)-\frac{\bar{\omega}k^2\pi[1+K'(k)-E'(k)]}{1-k^2}$$

where $\Pi\left[-(1-k^2),\sqrt{1-k^2},\frac{\pi}{2}\right]$ is a complete elliptic integral of the third kind with modulus $\sqrt{1-k^2}$ and parameter $-(1-k^2)$.

Summing all the various parts contributing to the third term in equation (C8), including the common factor, gives the following expression:

$$\frac{-1}{B(1-k^2)\sqrt{1+k^2}}\left\{\pi\tau k^3+\pi\bar{\omega}k^2+\frac{\pi K'(k)[2k^3\tau+\bar{\omega}k^2(1+k^2)]}{1-k^2}-\right.$$
$$\left.\frac{\pi E'(k)[2k^2\bar{\omega}+\tau k(1+k^2)]}{1-k^2}+\bar{\omega}k^2\pi(1-k^2)\Pi\left[-(1-k^2),1-k^2,\frac{\pi}{2}\right]\right\}\qquad\text{(C23)}$$

The addition of expression (C23) to expression (C9) completely evaluates ①. Expression (C3) gives the evaluation of ②, ③, and ④. Before writing the total integration, that is the sum of expressions (C23), (C9), and (C3), it is desirable to combine expressions (C3) and (C9), which are functions of Bm, and transform them by equation (C11) to functions of k. This procedure yields

$$\frac{\pi(\bar{\omega}k^2+\tau k^3)}{B\sqrt{1+k^2}(1-k^2)}\qquad\text{(C24)}$$

The total integration may now be written in terms of the parameter k as

$$\frac{-\pi}{B\sqrt{1+k^2}(1-k^2)^2}\left\{K'(k)[2k^3\tau+\bar{\omega}k^2(1+k^2)]-E'(k)[2k^2\bar{\omega}+\tau k(1+k^2)]+\bar{\omega}k^2(1-k^2)^2\Pi\left[-(1-k^2),1-k^2,\frac{\pi}{2}\right]\right\}\qquad\text{(C25)}$$

By use of the process commonly known as interchanging the amplitude and parameter (see pp. 133 to 141 of ref. 29) the elliptic integral of the third kind appearing in equation (C25) is found to be equivalent to $\frac{E'(k)}{k^2}$. This operation permits the expression for v/x (eq. (C25)) to assume the form given in equation (A20).

REFERENCES

1. Ribner, Herbert S.: The Stability Derivatives of Low-Aspect-Ratio Triangular Wings at Subsonic and Supersonic Speeds. NACA TN 1423, 1947.
2. Spreiter, John R.: The Aerodynamic Forces on Slender Plane- and Cruciform-Wing and Body Combinations. NACA Rep. 962, 1950. (Supersedes NACA TN's 1897 and 1662.)
3. Lomax, Harvard, and Heaslet, Max. A.: Damping-in-Roll Calculations for Slender Swept-Back Wings and Slender Wing-Body Combinations. NACA TN 1950, 1949.
4. Adams, Gaynor J.: Theoretical Damping in Roll and Rolling Effectiveness of Slender Cruciform Wings. NACA TN 2270, 1951.
5. Bobbitt, Percy J., and Malvestuto, Frank S., Jr.: Estimation of Forces and Moments Due to Rolling for Several Slender-Tail Configurations at Supersonic Speeds. NACA TN 2955, 1953.
6. Ribner, Herbert S.: Damping in Roll of Cruciform and Some Related Delta Wings at Supersonic Speeds. NACA TN 2285, 1951.
7. Martin, John C.: A Vector Study of Linearized Supersonic Flow Applications to Nonplanar Problems. NACA Rep. 1143, 1953. (Supersedes NACA TN 2641.)
8. Bleviss, Zegmund O.: Interference Effects in Supersonic Flow. Ph. D. Thesis, C.I.T., 1951.
9. Malvestuto, Frank S., Jr.: Theoretical Supersonic Force and Moment Coefficients on a Sideslipping Vertical- and Horizontal-Tail Combination With Subsonic Leading Edges and Supersonic Trailing Edges. NACA TN 3071, 1954.
10. Martin, John C., and Malvestuto, Frank S., Jr.: Theoretical Force and Moments Due to Sideslip of a Number of Vertical Tail Configurations at Supersonic Speeds. NACA TN 2412, 1951.
11. Heaslet, Max. A., Lomax, Harvard, and Jones, Arthur L.: Volterra's Solution of the Wave Equation as Applied to Three-Dimensional Supersonic Airfoil Problems. NACA Rep. 889, 1947. (Supersedes NACA TN 1412.)
12. Bryson, Arthur E., Jr.: Stability Derivatives for a Slender Missile With Application to a Wing-Body-Vertical-Tail Configuration. Jour. Aero. Sci., vol. 20, no. 5, May 1953, pp. 297–308.
13. Sacks, Alvin H.: Aerodynamic Forces, Moments, and Stability Derivatives for Slender Bodies of General Cross Section. NACA TN 3283, 1954.
14. Brown, Clinton E.: Theoretical Lift and Drag of Thin Triangular Wings at Supersonic Speeds. NACA Rep. 839, 1946. (Supersedes NACA TN 1183.)
15. Brown, Clinton E., and Adams, Mac C.: Damping in Pitch and Roll of Triangular Wings at Supersonic Speeds. NACA Rep 892, 1948. (Supersedes NACA TN 1566.)
16. Evvard, John C.: Distribution of Wave Drag and Lift in the Vicinity of Wing Tips at Supersonic Speeds. NACA TN 1382, 1947.
17. Malvestuto, Frank S., Jr., Margolis, Kenneth, and Ribner, Herbert S.: Theoretical Lift and Damping in Roll at Supersonic Speeds of Thin Sweptback Tapered Wings With Streamwise Tips, Subsonic Leading Edges, and Supersonic Trailing Edges. NACA Rep. 970, 1950. (Supersedes NACA TN 1860.)
18. Martin, John C., Margolis, Kenneth, and Jeffreys, Isabella: Calculation of Lift and Pitching Moments Due to Angle of Attack and Steady Pitching Velocity at Supersonic Speeds for Thin Sweptback Tapered Wings With Streamwise Tips and Supersonic Leading and Trailing Edges. NACA TN 2699, 1952.
19. Margolis, Kenneth, Sherman, Windsor L., and Hannah, Margery E.: Theoretical Calculation of the Pressure Distribution, Span Loading, and Rolling Moment Due to Sideslip at Supersonic Speeds for Thin Sweptback Tapered Wings With Supersonic Trailing Edges and Wing Tips Parallel to the Axis of Wing Symmetry. NACA TN 2898, 1953.
20. Harmon, Sidney M., and Jeffreys, Isabella: Theoretical Lift and Damping in Roll of Thin Wings With Arbitrary Sweep and Taper at Supersonic Speeds—Supersonic Leading and Trailing Edges. NACA TN 2114, 1950.
21. Ribner, Herbert S., and Malvestuto, Frank S., Jr: Stability Derivatives of Triangular Wings at Supersonic Speeds. NACA Rep. 908, 1948. (Supersedes NACA TN 1572.)
22. Malvestuto, Frank S., Jr., and Hoover, Dorothy M.: Supersonic Lift and Pitching Moment of Thin Sweptback Tapered Wings

Produced by Constant Vertical Acceleration—Subsonic Leading Edges and Supersonic Trailing Edges. NACA TN 2315, 1951.

23. Cole, Isabella J., and Margolis, Kenneth: Lift and Pitching Moment at Supersonic Speeds Due to Constant Vertical Acceleration for Thin Sweptback Tapered Wings With Streamwise Tips—Supersonic Leading and Trailing Edges. NACA TN 3196, 1954.

24. Malvestuto, Frank S., Jr., and Margolis, Kenneth: Theoretical Stability Derivatives of Thin Sweptback Wings Tapered to a Point With Sweptback or Sweptforward Trailing Edges for a Limited Range of Supersonic Speeds. NACA Rep. 971, 1950.

(Supersedes NACA TN 1761).

25. Busemann, Adolf: Infinitesimal Conical Supersonic Flow. NACA TM 1100, 1947.

26. Lomax, Harvard, and Heaslet, Max. A.: Generalized Conical-Flow Fields in Supersonic Wing Theory. NACA TN 2497, 1951.

27. Peirce, B. O.: A Short Table of Integrals. Third rev. ed., Ginn and Co., 1929.

28. De Haan, D. Bierens: Nouvelles Tables D'Intégrales Définies. G. E. Stechart & Co. (New York), 1939, pp. 475–477.

29. Cayley, Arthur: An Elementary Treatise on Elliptic Functions. Second ed., George Bell and Sons (London), 1895.

TABLE I

FORMULAS FOR POTENTIAL DISTRIBUTION DUE TO CONSTANT SIDESLIP
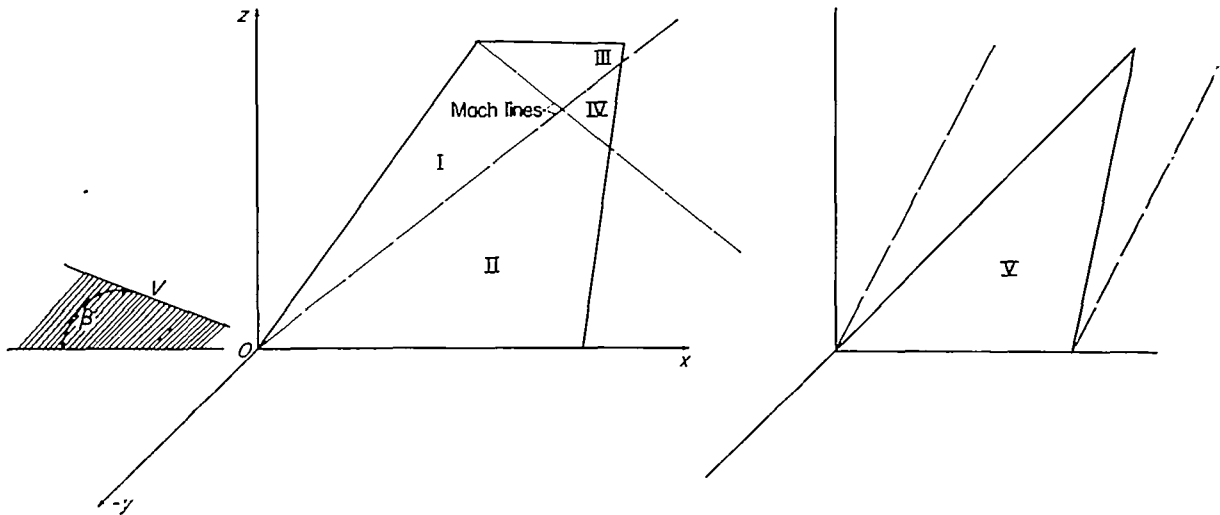
(Tail is in xz-plane; β is positive; V as shown is in xy-plane)

Region (see sketch)	$\varphi(x,0^+,z)$
I	$-\dfrac{V\beta(mx-z)}{\sqrt{B^2m^2-1}}$
II	$-\dfrac{V\beta}{\pi\sqrt{B^2m^2-1}}\left[(mx-z)\cos^{-1}\dfrac{mx-z(2Bm-1)}{mx-z}+2\sqrt{zm(x-Bz)(Bm-1)}\right]$
III	$-\dfrac{V\beta}{\pi\sqrt{B^2m^2-1}}\left\{(mx-z)\cos^{-1}\dfrac{mx-z+2(1+Bm)(z-b)}{mx-z}+2\sqrt{(z-b)(Bm+1)[b(1+Bm)-m(x+Bz)]}\right\}$
IV	Σ (II+III−I)
V	$-\dfrac{V\beta H(Bm)\sqrt{z(mx-z)}}{Bm}$

TABLE II

FORMULAS FOR PRESSURE-DIFFERENCE COEFFICIENT DUE TO CONSTANT SIDESLIP
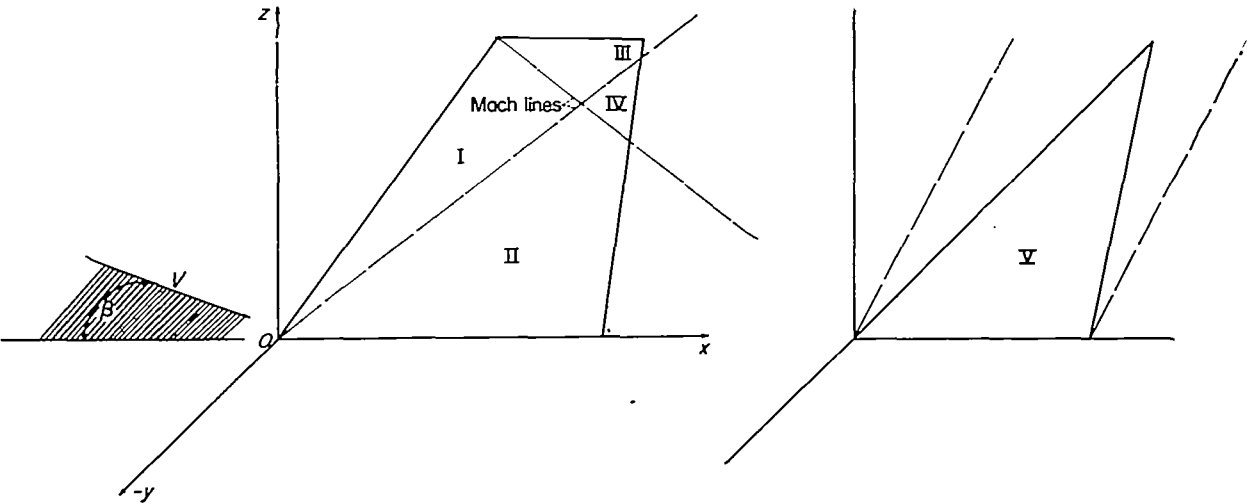
(Tail is in xz-plane; β is positive; V as shown is in xy-plane)

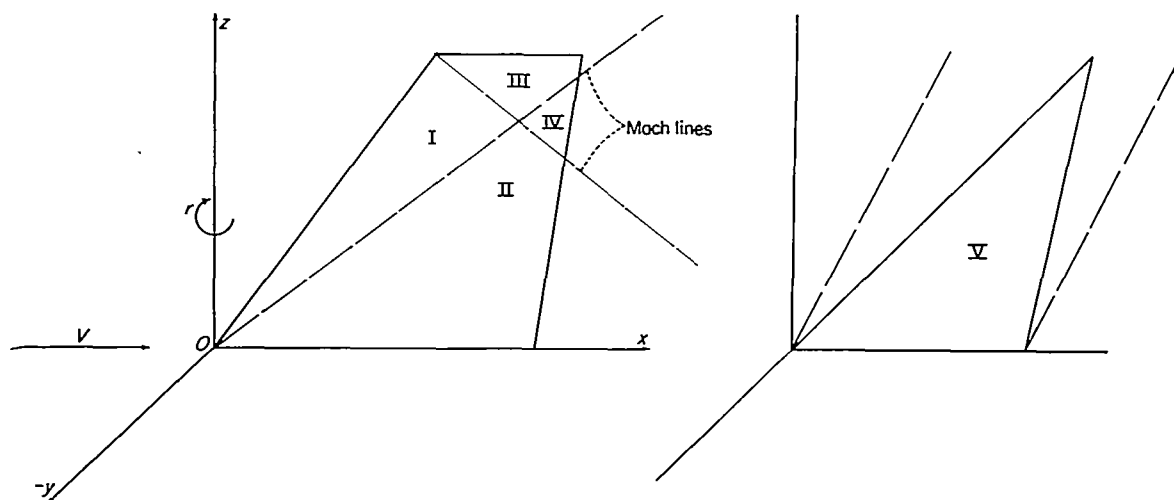| Region (see sketch)	$\dfrac{\Delta P}{q}\,(x,z)$
I	$-\dfrac{4\beta m}{\sqrt{B^2 m^2 - 1}}$
II	$-\dfrac{4\beta m}{\pi\sqrt{B^2 m^2 - 1}}\cos^{-1}\dfrac{mx - z(2Bm - 1)}{mx - z}$
III	$-\dfrac{4\beta m}{\pi\sqrt{B^2 m^2 - 1}}\cos^{-1}\dfrac{mx - z + 2(1 + Bm)(z - b)}{mx - z}$
IV	$\Sigma\,(\mathrm{II} + \mathrm{III} - \mathrm{I})$
V	$-\dfrac{2\beta z H(Bm)}{B\sqrt{z(mx - z)}}$

TABLE III
FORMULAS FOR POTENTIAL DISTRIBUTION DUE TO STEADY ROLLING
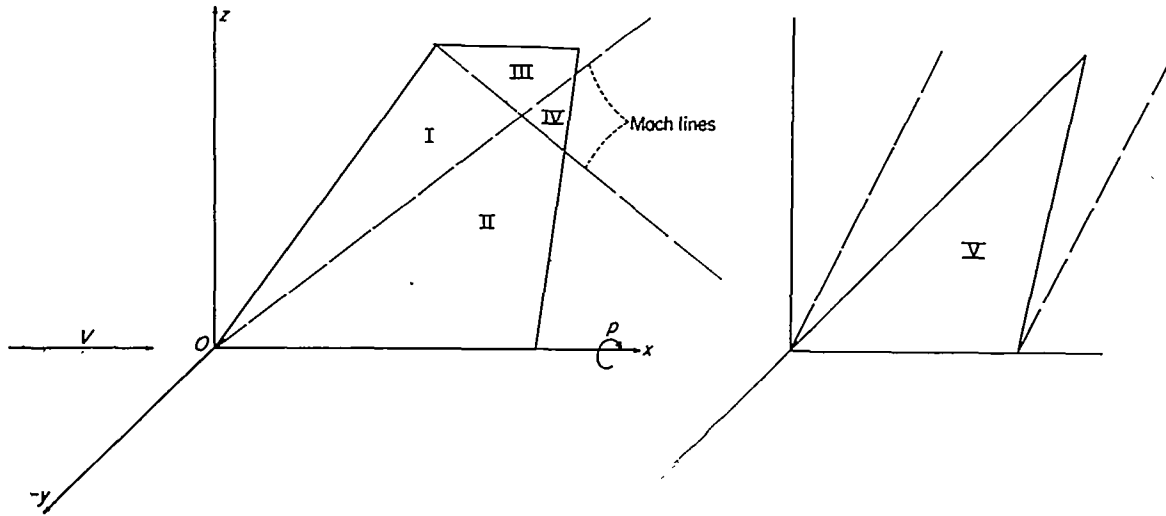
(Tail is in xz-plane; positive rolling)

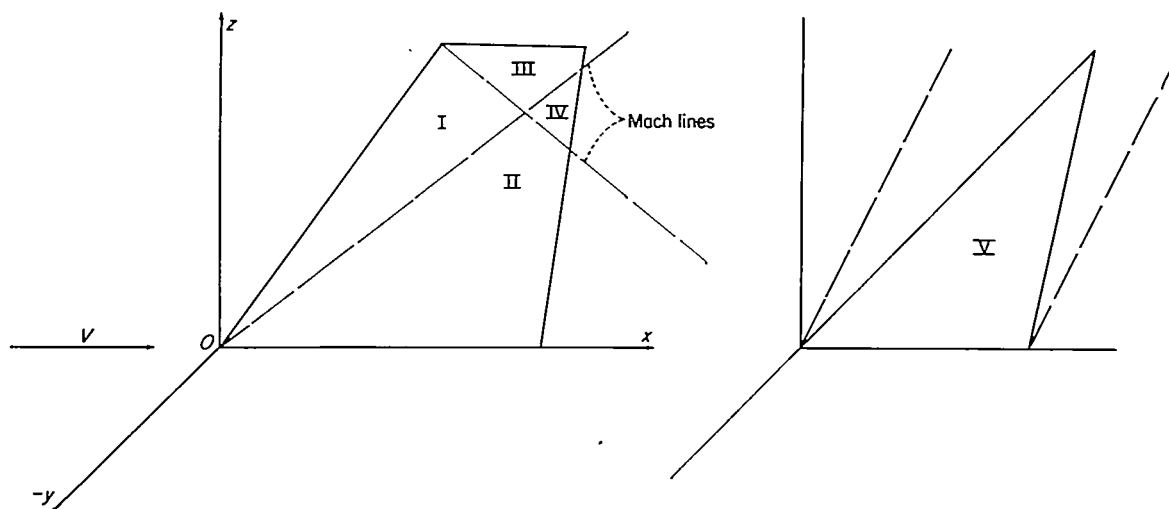| Region (see sketch)	$\varphi(x,0^+,z)$
I	$-\dfrac{p}{2(B^2m^2-1)^{3/2}}\left\{(mx-z)[-mx+z(2B^2m^2-1)]\right\}$
II	$-\dfrac{p}{\pi}\left\{\dfrac{mx(4Bm-1)+z(2B^2m^2-2Bm-3)}{3(B^2m^2-1)}\sqrt{\dfrac{mz(x-Bz)}{Bm+1}}-\dfrac{(mx-z)[mx-z(2B^2m^2-1)]}{2(B^2m^2-1)^{3/2}}\cos^{-1}\dfrac{mx+z(1-2Bm)}{mx-z}\right\}$
III	$-\dfrac{p}{\pi(B^2m^2-1)^{3/2}}\left\{\dfrac{(mx-z)[-mx+z(2B^2m^2-1)]}{2}\cos^{-1}\dfrac{mx-z+2(1+Bm)(z-b)}{mx-z}-\dfrac{(mx-b)(4Bm-1)+(z-b)(3-2B^2m^2-2Bm)-6b(B^2m^2-1)}{3}\sqrt{(z-b)(Bm+1)[b(1+Bm)-m(x+Bz)]}\right\}$
IV	$\Sigma(\text{II}+\text{III}-\text{I})$
V	$p(\tau_p'z+\omega_p'mx)\sqrt{z(mx-z)}$

TABLE IV

FORMULAS FOR PRESSURE-DIFFERENCE COEFFICIENT DUE TO STEADY ROLLING
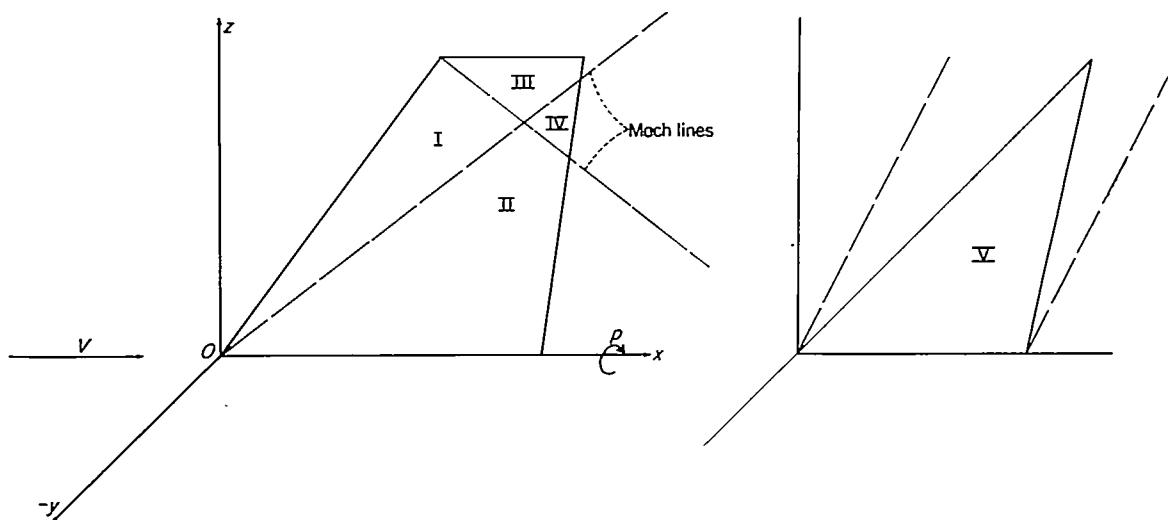
(Tail is in xz-plane; positive rolling)

Region (see sketch)	$\dfrac{\Delta P}{q}(x,z)$
I	$-\dfrac{4pm(B^2m^2z-mx)}{V(B^2m^2-1)^{3/2}}$
II	$-\dfrac{4p}{\pi V}\left[\dfrac{2Bm^2}{(B^2m^2-1)}\sqrt{\dfrac{zm(x-Bz)}{Bm+1}}-\dfrac{m^2(x-B^2zm)}{(B^2m^2-1)^{3/2}}\cos^{-1}\dfrac{mx+z(1-2Bm)}{mx-z}\right]$
III	$-\dfrac{4pm}{\pi V(B^2m^2-1)^{3/2}}\left\{(B^2m^2z-mx)\cos^{-1}\dfrac{mx-z+2(1+Bm)(z-b)}{mx-z}-2Bm\sqrt{(z-b)(Bm+1)[b(1+Bm)-m(x+Bz)]}\right\}$
IV	$\Sigma(\mathrm{II+III-I})$
V	$\dfrac{2p}{V}\dfrac{\tau_p{}'mz^2+3m^2\omega_p{}'xz-2m\omega_p{}'z^2}{\sqrt{z(mx-z)}}$

TABLE V

FORMULAS FOR POTENTIAL DISTRIBUTION DUE TO STEADY YAWING

(Tail is in xz-plane; positive yawing)

Region (see sketch)	$\varphi(x,0^+,z)$
I	$\dfrac{r}{2(B^2m^2-1)^{3/2}}\,[x^2(-2m+B^2m^3)+2xz-B^2z^2m]$
II	$\dfrac{r}{\pi}\left\{\dfrac{x(5B^2m^2+4Bm-6)-B^2mz(2Bm+1)}{3(B^2m^2-1)}\sqrt{\dfrac{mz(x-Bz)}{Bm+1}}+\right.$ $\left.\dfrac{(mx-z)[mzB^2+x(m^2B^2-2)]}{2(B^2m^2-1)^{3/2}}\cos^{-1}\dfrac{mx-z(2Bm-1)}{mx-z}\right\}$
III	$\dfrac{r}{\pi}\left\{\dfrac{mx(5B^2m^2-4Bm-6)+B^2m^2(z-b)(2Bm-1)+Bmb(4+Bm)}{3m(B^2m^2-1)^{3/2}}\sqrt{(z-b)(Bm+1)[b(1+Bm)-m(x+Bz)]}+\right.$ $\left.\dfrac{(mx-z)[B^2m^2(mx+z)-2mx]}{2m(B^2m^2-1)^{3/2}}\cos^{-1}\dfrac{mx-z+2(1+Bm)(z-b)}{mx-z}\right\}$
IV	$\Sigma(\text{II}+\text{III}-\text{I})$
V	$Br(\tau_r'z+\omega_r'mx)\sqrt{z(mx-z)}$

TABLE VI

FORMULAS FOR PRESSURE-DIFFERENCE COEFFICIENT DUE TO STEADY YAWING

(Tail is in xz-plane; positive yawing)

Region (see sketch)	$\dfrac{\Delta P}{q}(x,z)$
I	$\dfrac{4r}{V(B^2m^2-1)^{3/2}}\,[mx(B^2m^2-2)+z]$
II	$\dfrac{4r}{\pi V(B^2m^2-1)^{3/2}}\left\{[mx(B^2m^2-2)+z]\cos^{-1}\dfrac{mx-z(2Bm-1)}{mx-z}+2(B^2m^2+Bm-1)\sqrt{mz(Bm-1)(x-Bz)}\right\}$
III	$\dfrac{4r}{\pi V(B^2m^2-1)^{3/2}}\left\{[z+mx(B^2m^2-2)]\cos^{-1}\dfrac{mx-z+2(1+Bm)(z-b)}{mx-z}+2(B^2m^2-Bm-1)\sqrt{(z-b)(Bm+1)[b(1+Bm)-m(x+Bz)]}\right\}$
IV	$\Sigma(\text{II}+\text{III}-\text{I})$
V	$\dfrac{2Br}{V}\dfrac{\tau_r' mz^2+3m^2\omega_r' xz-2m\omega_r' z^2}{\sqrt{z(mx-z)}}$

TABLE VII
FORMULAS FOR POTENTIAL DISTRIBUTION DUE TO CONSTANT LATERAL ACCELERATION

(Tail is in xz-plane; positive $\dot{\beta}$ in positive y-direction)

Region (see sketch)	$\varphi(x,0^+,z)$
I	$-\dfrac{\dot{\beta}\,(mx-z)}{\sqrt{B^2m^2-1}}\left[tV-\dfrac{mM^2(mx-z)}{2(B^2m^2-1)}\right]$
II	$-\dfrac{\dot{\beta}}{\pi\sqrt{B^2m^2-1}}\left\{\sqrt{mz(x-Bz)(Bm-1)}\left[2tV+\dfrac{M^2mx(4-Bm)-M^2mBz(2Bm+1)}{3B(B^2m^2-1)}\right]+\right.$ $\left.\left[\cos^{-1}\dfrac{mx-z(2Bm-1)}{mx-z}\right]\left[\dfrac{M^2m(z-mx)}{2(B^2m^2-1)}+tV\right](mx-z)\right\}$
III	$-\dfrac{\dot{\beta}}{\pi\sqrt{B^2m^2-1}}\left\{\sqrt{(z-b)(Bm+1)[b(1+Bm)-m(x+Bz)]}\left[2tV+\dfrac{M^2(4+Bm)(b-mx)+M^2Bm(z-b)(2Bm-1)}{3B(B^2m^2-1)}\right]+\right.$ $\left.\left[\cos^{-1}\dfrac{mx-z+2(1+Bm)(z-b)}{mx-z}\right]\left[tV+\dfrac{M^2m(z-mx)}{2(B^2m^2-1)}\right](mx-z)\right\}$
IV	$\Sigma(\text{II}+\text{III}-\text{I})$
V	$-\dot{\beta}\sqrt{z(mx-z)}\left\{\dfrac{(B^2+1)}{B}\,(\tau_r'z+\omega_r'mx)+\left[Vt-\dfrac{(B^2+1)x}{B^2}\right]\dfrac{H(Bm)}{Bm}\right\}$

TABLE VIII

FORMULAS FOR PRESSURE-DIFFERENCE COEFFICIENT DUE TO CONSTANT LATERAL ACCELERATION
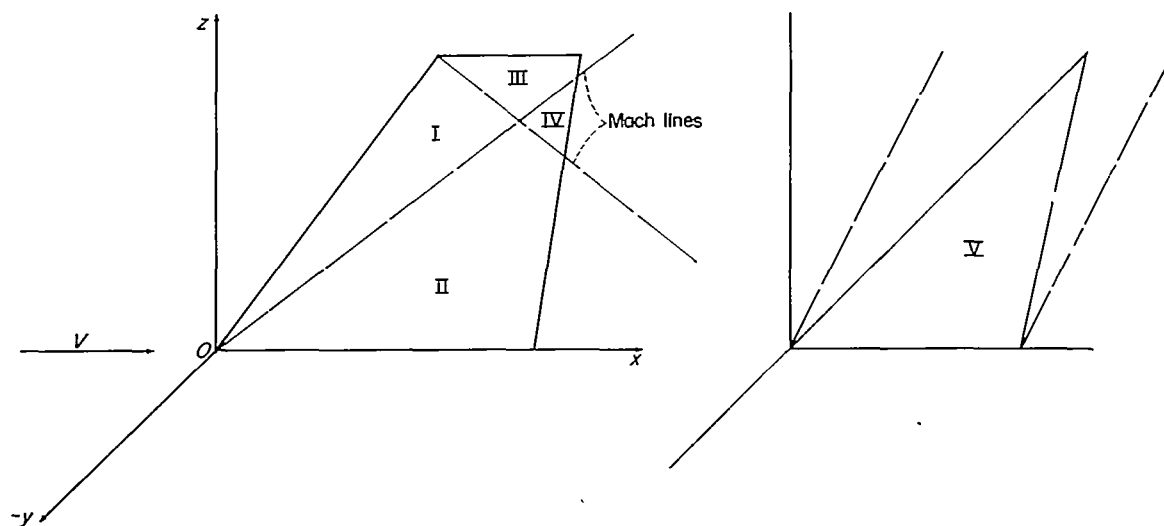
(Tail is in xz-plane; positive $\dot{\beta}$ in positive y-direction)

Region (see sketch)	$\dfrac{\Delta P}{q}(x,z)$
I	$\dfrac{4\dot{\beta}(mx-z)(1+m^2)}{V(B^2m^2-1)^{3/2}}$
II	$\dfrac{4\dot{\beta}}{\pi B^2 V\sqrt{B^2m^2-1}}\left\{\dfrac{B^2(1+m^2)(mx-z)}{B^2m^2-1}\cos^{-1}\dfrac{mx-z(2Bm-1)}{mx-z}+\right.$ $\left. 2\left[1-\dfrac{M^2(B^2m^2+Bm-1)}{B^2m^2-1}\right]\sqrt{zm(x-Bz)(Bm-1)}\right\}$
III	$\dfrac{4\dot{\beta}}{\pi B^2 V\sqrt{B^2m^2-1}}\left\{\dfrac{B^2(1+m^2)(mx-z)}{B^2m^2-1}\cos^{-1}\dfrac{mx-z+2(1+Bm)(z-b)}{mx-z}+\right.$ $\left. 2\left[1-\dfrac{M^2(B^2m^2-Bm-1)}{B^2m^2-1}\right]\sqrt{(z-b)(Bm+1)[b(1+Bm)-m(x+Bz)]}\right\}$
IV	$\Sigma(\text{II}+\text{III}-\text{I})$
V	$-\dfrac{2\dot{\beta}}{B^2\bar{V}}\left[\dfrac{(B^2+1)B(\tau_r{}'mz^2+3m^2\omega_r{}'xz-2m\omega_r{}'z^2)}{\sqrt{z(mx-z)}}-\right.$ $\left. \dfrac{(B^2+1)xzH(Bm)}{B\sqrt{z(mx-z)}}-\dfrac{2H(Bm)\sqrt{z(mx-z)}}{Bm}\right]$

TABLE IX
STABILITY DERIVATIVES FOR HALF-DELTA AND RECTANGULAR ISOLATED VERTICAL TAILS

Derivative (a)	Half-delta tails		Rectangular tails $AB \geq 1$
	$0 \leq AB < 2$	$AB \geq 2$	
C_{Y_β}	$-\dfrac{\pi}{B} H(Bm)$	$-\dfrac{4}{B}\sqrt{\dfrac{AB}{AB+2}}$	$-\dfrac{4}{B}\left(1-\dfrac{1}{2AB}\right)$
C_{n_β}	$\dfrac{4\pi}{3AB} H(Bm)$	$\dfrac{16}{3AB}\sqrt{\dfrac{AB}{AB+2}}$	$\dfrac{2}{AB}\left(1-\dfrac{2}{3AB}\right)$
C_{l_β}	$-\dfrac{\pi}{2B} H(Bm)$	$-\dfrac{4}{3B}\dfrac{AB+1}{\sqrt{AB(AB+2)}}$	$-\dfrac{2}{B}\left(1-\dfrac{1}{2AB}\right)$
C_{Y_p}	$\dfrac{\pi AB}{4B}(\tau_p'+2\omega_p')$	$-\dfrac{4}{3B}\dfrac{\sqrt{AB}(AB+3)}{(AB+2)^{3/2}}$	$-\dfrac{2AB-1}{AB^2}$
C_{n_p}	$-\dfrac{3\pi}{8}(\tau_p'+2\omega_p')$	$\dfrac{2(AB+3)}{\sqrt{AB}(AB+2)^{3/2}}$	$\dfrac{3AB-2}{3A^2B^2}$
C_{l_p}	$\dfrac{\pi AB}{4B}\left(\dfrac{5}{8}\tau_p'+\omega_p'\right)$	$-\dfrac{2A^2B^2+6AB+3}{3B\sqrt{AB}(AB+2)^{3/2}}$	$-\dfrac{1+4AB-24A^2B^2+32A^3B^3}{24A^3B^4}$
C_{Y_r}	$\dfrac{\pi AB}{4}(\tau_r'+2\omega_r')$	$\dfrac{8(2AB+5)}{3\sqrt{AB}(AB+2)^{3/2}}$	$\dfrac{2(3AB-1)}{3A^2B^2}$
C_{n_r}	$-\dfrac{3\pi B}{8}(\tau_r'+2\omega_r')$	$-\dfrac{4B(2AB+5)}{[AB(AB+2)]^{3/2}}$	$-\dfrac{B(8AB-3)}{6A^3B^3}$
C_{l_r}	$\dfrac{\pi AB}{4}\left(\dfrac{5}{8}\tau_r'+\omega_r'\right)$	$\dfrac{2(3A^2B^2+9AB+5)}{3[AB(AB+2)]^{3/2}}$	$\dfrac{3AB-1}{3A^2B^2}$
$C_{Y_{\dot\beta}}$	$-\dfrac{AB\pi}{4}\left[\tau_r'+2\omega_r'-\dfrac{16H(Bm)}{3A^2B^2}\right]-\dfrac{AB\pi}{4B^2}\left[\tau_r'+2\omega_r'-\dfrac{8H(Bm)}{A^2B^2}\right]$	$-\dfrac{8}{3B^2}\dfrac{B^2-AB-1}{\sqrt{AB(AB+2)^3}}$	$-\dfrac{2(B^2+2-3AB)}{3A^2B^4}$
$C_{n_{\dot\beta}}$	$\dfrac{\pi B}{4}\left[\dfrac{3}{2}\tau_r'+3\omega_r'-\dfrac{8H(Bm)}{A^2B^2}\right]+\dfrac{\pi}{4B}\left[\dfrac{3}{2}\tau_r'+3\omega_r'-\dfrac{12H(Bm)}{A^2B^2}\right]$	$\dfrac{4}{B}\dfrac{B^2-AB-1}{\sqrt{A^2B^3(AB+2)^3}}$	$\dfrac{3B^2-8AB+6}{6A^3B^4}$
$C_{l_{\dot\beta}}$	$-\dfrac{AB\pi}{8}\left[2\omega_r'+\dfrac{5}{4}\tau_r'-\dfrac{6H(Bm)}{A^2B^2}\right]-\dfrac{AB\pi}{8B^2}\left[2\omega_r'+\dfrac{5}{4}\tau_r'-\dfrac{8H(Bm)}{A^2B^2}\right]$	$\dfrac{2}{3B^2}\dfrac{B^2+A^2B^2+3AB+3}{\sqrt{A^2B^3(AB+2)^3}}$	$-\dfrac{B^2+2-3AB}{3A^2B^4}$

a Angular velocities and moments measured about the system of body axes shown in figure 2 (b).

TABLE X

STABILITY DERIVATIVES FOR TRIANGULAR ISOLATED VERTICAL TAILS
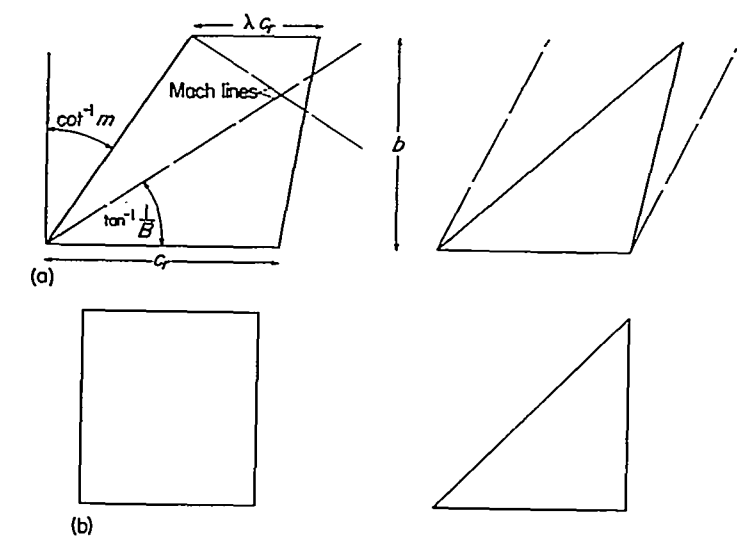WITH SUBSONIC LEADING EDGE AND SUPERSONIC TRAILING EDGE

Derivative (a)	Formula (b)
C_{Y_β}	$-\dfrac{\pi}{B}\sqrt{\dfrac{AB}{2Bm}}\,H(Bm)$
C_{n_β}	$\dfrac{\pi(3AB+2Bm)}{6Bm\sqrt{2BmAB}}\,H(Bm)$
C_{l_β}	$-\dfrac{\pi}{2B}\sqrt{\dfrac{AB}{2Bm}}\,H(Bm)$
C_{Y_p}	$\dfrac{\pi}{B}\sqrt{2BmAB}\left(\dfrac{\tau_p{}'}{4}+\dfrac{\omega_p{}'}{4}+\dfrac{Bm}{2AB}\,\omega_p{}'\right)$
C_{n_p}	$-\pi\sqrt{2BmAB}\left[\tau_p{}'\left(\dfrac{5}{32Bm}+\dfrac{1}{16AB}\right)+\omega_p{}'\left(\dfrac{5}{32Bm}+\dfrac{1}{4AB}+\dfrac{3Bm}{8A^2B^2}\right)\right]$
C_{l_p}	$\dfrac{\pi}{16B}\sqrt{2BmAB}\left(\dfrac{5}{2}\tau_p{}'+\dfrac{5}{2}\omega_p{}'+\dfrac{3Bm}{AB}\,\omega_p{}'\right)$
C_{Y_r}	$\pi\sqrt{2BmAB}\left(\dfrac{\tau_r{}'}{4}+\dfrac{\omega_r{}'}{4}+\dfrac{Bm}{2AB}\,\omega_r{}'\right)$
C_{n_r}	$-\pi B\sqrt{2BmAB}\left[\tau_r{}'\left(\dfrac{5}{32Bm}+\dfrac{1}{16AB}\right)+\omega_r{}'\left(\dfrac{5}{32Bm}+\dfrac{1}{4AB}+\dfrac{3Bm}{8A^2B^2}\right)\right]$
C_{l_r}	$\dfrac{\pi}{16}\sqrt{2BmAB}\left(\dfrac{5}{2}\tau_r{}'+\dfrac{5}{2}\omega_r{}'+\dfrac{3Bm}{AB}\,\omega_r{}'\right)$
$C_{Y_{\dot\beta}}$	$-\pi\sqrt{2BmAB}\left[\dfrac{\tau_r{}'}{4}+\dfrac{\omega_r{}'}{4}\left(1+\dfrac{2Bm}{AB}\right)-\dfrac{H(Bm)}{4B^2m^2}-\dfrac{H(Bm)}{6BmAB}\right]-$ $\dfrac{\pi}{B^2}\sqrt{2BmAB}\left[\dfrac{\tau_r{}'}{4}+\dfrac{\omega_r{}'}{4}\left(1+\dfrac{2Bm}{AB}\right)-\dfrac{H(Bm)}{4B^2m^2}-\dfrac{H(Bm)}{2BmAB}\right]$
$C_{n_{\dot\beta}}$	$\pi B\sqrt{2BmAB}\left[\tau_r{}'\left(\dfrac{5}{32Bm}+\dfrac{1}{16AB}\right)+\omega_r{}'\left(\dfrac{5}{32Bm}+\dfrac{1}{4AB}+\dfrac{3Bm}{8A^2B^2}\right)-\right.$ $\left.\left(\dfrac{5}{32B^3m^3}+\dfrac{1}{8B^2m^2AB}+\dfrac{1}{8BmA^2B^2}\right)H(Bm)\right]+$ $\dfrac{\pi}{B}\sqrt{2BmAB}\left[\tau_r{}'\left(\dfrac{5}{32Bm}+\dfrac{1}{16AB}\right)+\omega_r{}'\left(\dfrac{5}{32Bm}+\dfrac{1}{4AB}+\dfrac{3Bm}{8A^2B^2}\right)-\right.$ $\left.\left(\dfrac{5}{32B^3m^3}+\dfrac{1}{4B^2m^2AB}+\dfrac{3}{8BmA^2B^2}\right)H(Bm)\right]$
$C_{l_{\dot\beta}}$	$-\dfrac{\pi}{32}\sqrt{2BmAB}\left[5\tau_r{}'+5\omega_r{}'+\dfrac{6Bm}{AB}\,\omega_r{}'-\left(\dfrac{5}{B^2m^2}+\dfrac{2}{BmAB}\right)H(Bm)\right]-$ $\dfrac{\pi}{32B^2}\sqrt{2BmAB}\left[5\tau_r{}'+5\omega_r{}'+\dfrac{6Bm}{AB}\,\omega_r{}'-\left(\dfrac{5}{B^2m^2}+\dfrac{6}{BmAB}\right)H(Bm)\right]$

ᵃ Angular velocities and moments measured about the system of body axes shown in figure 2 (b).
ᵇ Formulas valid for triangular plan forms with either sweptback or sweptforward trailing edge provided the edge is supersonic.

TABLE XI

TRANSFER-OF-AXES FORMULAS

Stability derivatives in a body system of axes with origin at tail apex (see fig. 2 (b))	Formulas for transfer to a body system of axes with origin displaced distances x_0 (positive forward) and z_0 (positive downward) from the tail apex (see fig. 2 (c))
C_{Y_β}	C_{Y_β}
C_{n_β}	$C_{n_\beta}-\dfrac{x_0}{b}\,C_{Y_\beta}$
C_{l_β}	$C_{l_\beta}+\dfrac{z_0}{b}\,C_{Y_\beta}$
C_{Y_p}	C_{Y_p}
C_{n_p}	$C_{n_p}-\dfrac{x_0}{b}\,C_{Y_p}$
C_{l_p}	$C_{l_p}+\dfrac{z_0}{b}\,C_{Y_p}$
C_{Y_r}	$C_{Y_r}-\dfrac{x_0}{b}\,C_{Y_\beta}$
C_{n_r}	$C_{n_r}-\dfrac{x_0}{b}\left(C_{n_\beta}+C_{Y_r}\right)+\left(\dfrac{x_0}{b}\right)^2 C_{Y_\beta}$
C_{l_r}	$C_{l_r}+\dfrac{z_0}{b}\,C_{Y_r}-\dfrac{x_0}{b}\,C_{l_\beta}-\left(\dfrac{z_0}{b}\right)\left(\dfrac{x_0}{b}\right)C_{Y_\beta}$
$C_{Y_{\dot\beta}}$	$C_{Y_{\dot\beta}}$
$C_{n_{\dot\beta}}$	$C_{n_{\dot\beta}}-\dfrac{x_0}{b}\,C_{Y_{\dot\beta}}$
$C_{l_{\dot\beta}}$	$C_{l_{\dot\beta}}+\dfrac{z_0}{b}\,C_{Y_{\dot\beta}}$

(a) Plan forms of vertical tails analyzed. (Trailing edge may be either sweptback or sweptforward provided it remains supersonic.)

(b) Special cases (rectangular and half-delta vertical tails) for which stability-derivative curves are presented.

FIGURE 1.—Tail plan forms and associated data.
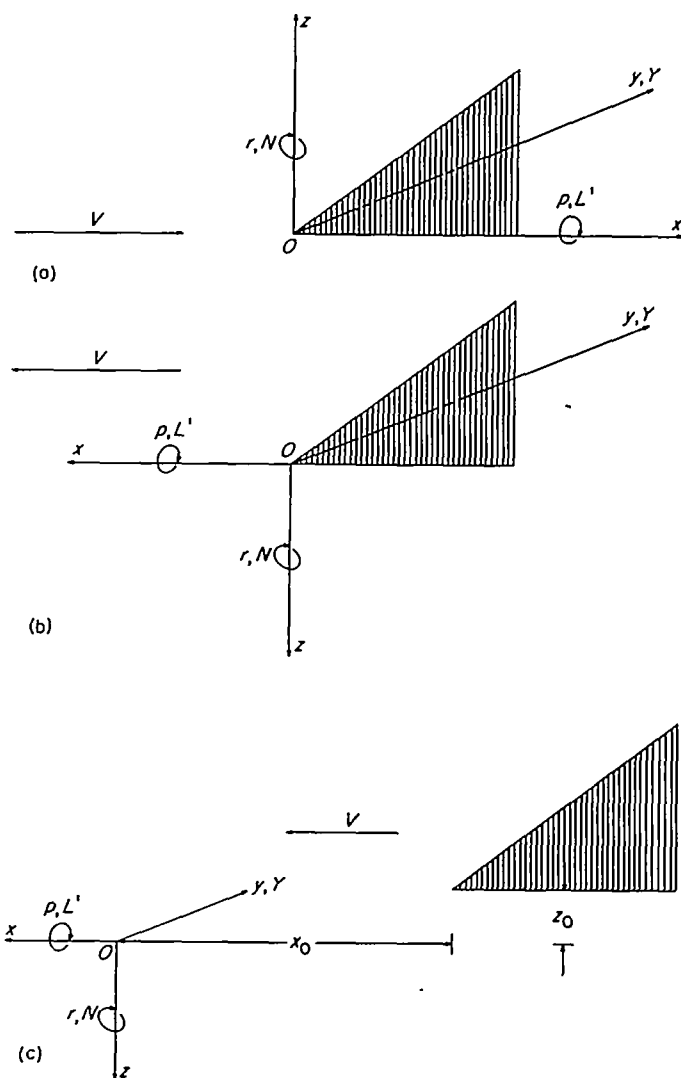
(a) Body-axes system used for analysis. Free-stream velocity V.

(b) Principal body-axes system used for presentation of stability derivatives. Entire system moving with flight velocity V.

(c) Same type of axes system as (b) with origin translated.

FIGURE 2.—Systems of body axes. Positive directions of axes, forces, and moments indicated by arrows.
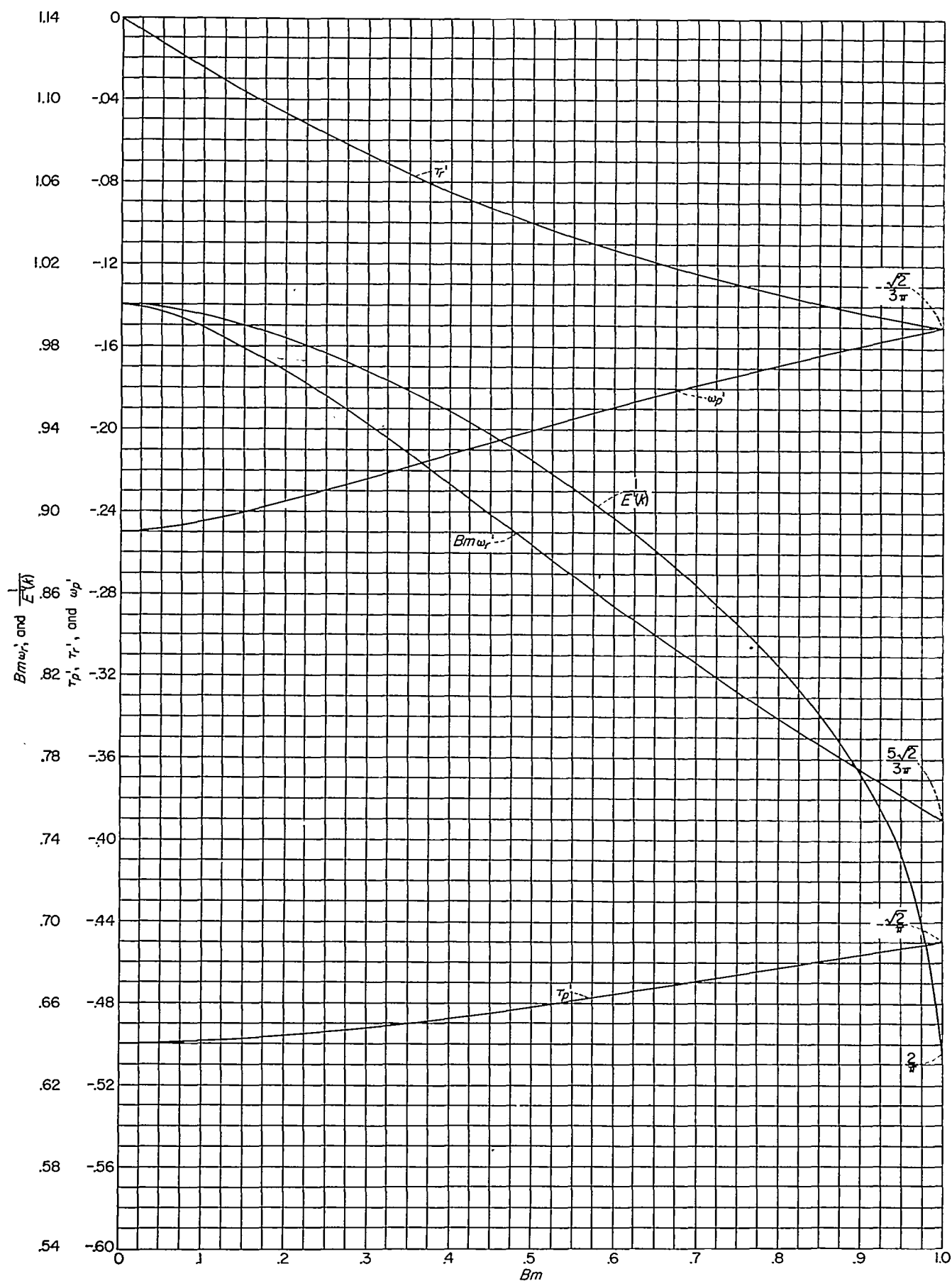
FIGURE 3.—Variation of the parameters $\dfrac{1}{E'(k)}$, $\omega_p{}'$, $Bm\omega_r{}'$, $\tau_p{}'$ and $\tau_r{}'$ with Bm.
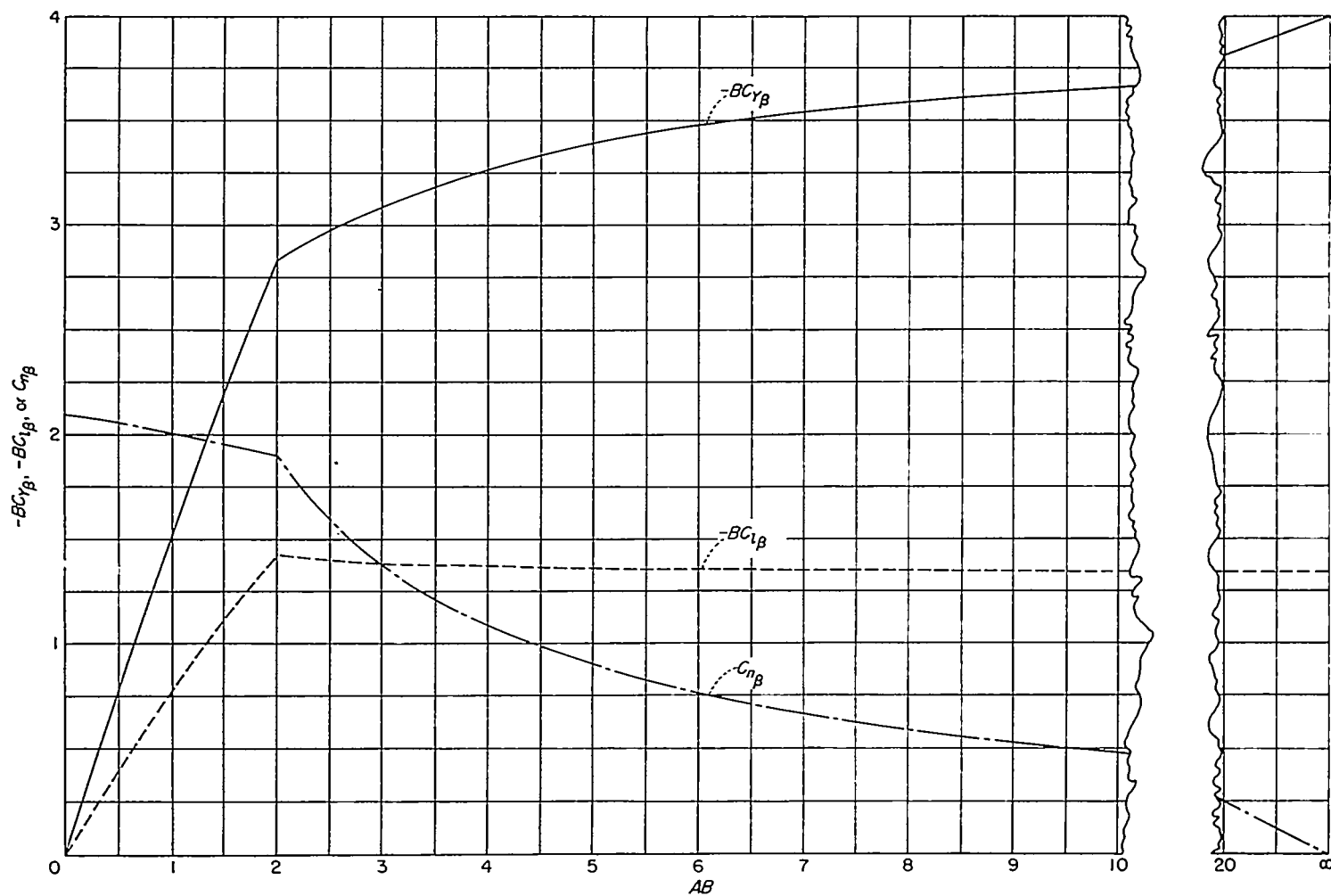
FIGURE 4.—Curves for determining the stability derivatives due to constant sideslip C_{Y_β}, C_{n_β}, and C_{l_β} for isolated half-delta vertical tails. Derivatives based on vertical-tail parameters b and S; principal body-axes system with origin at leading edge of root section.
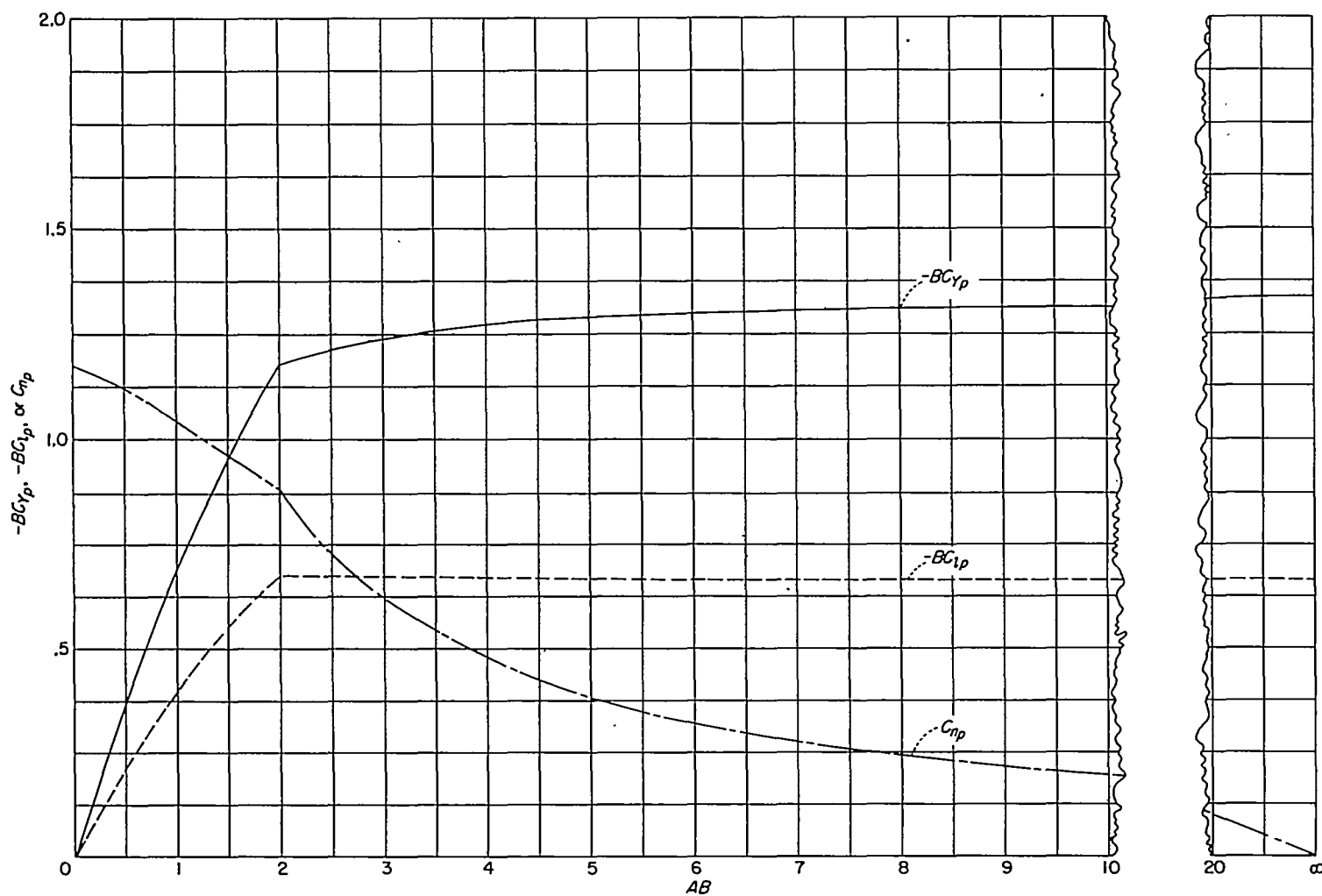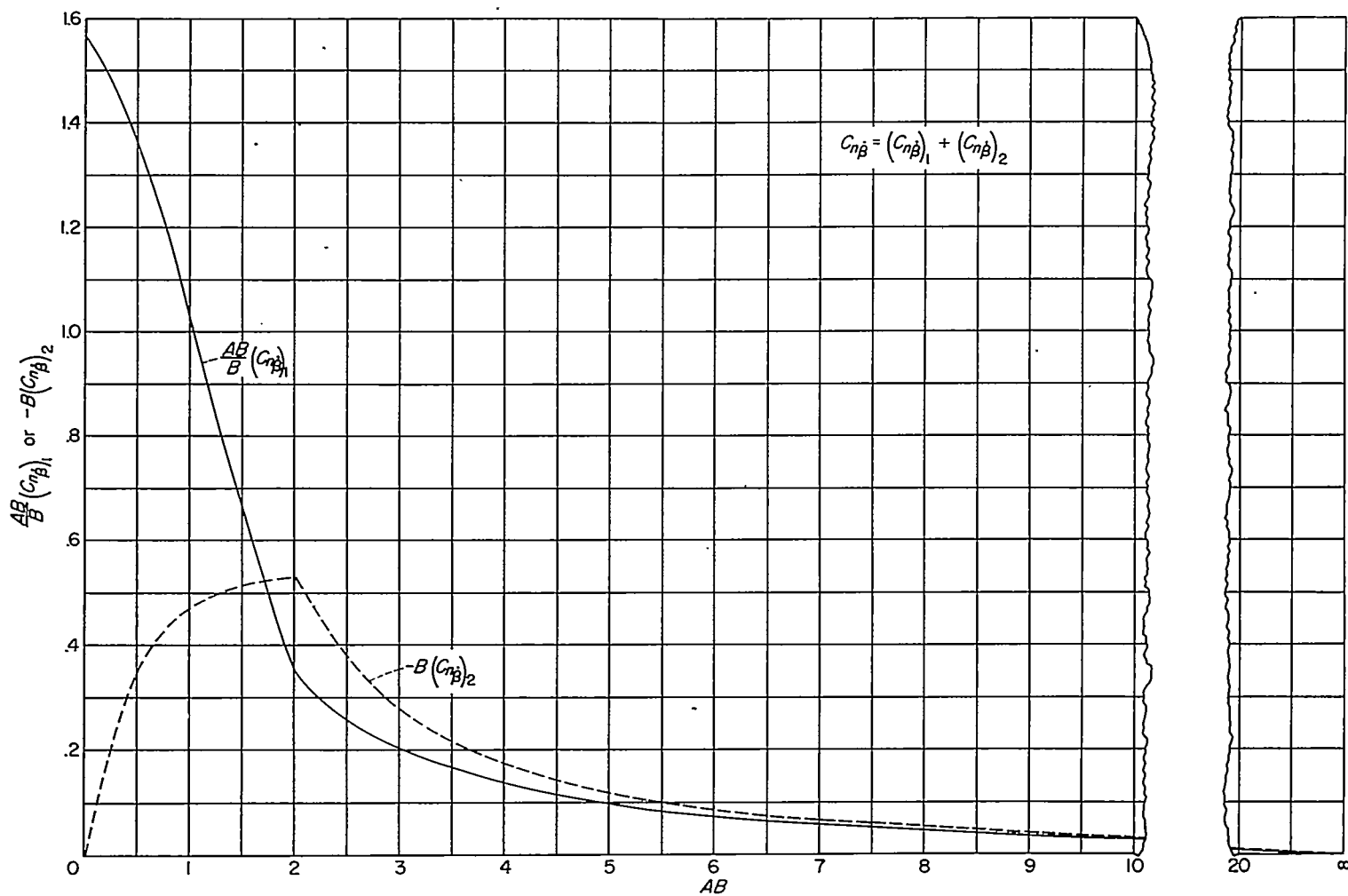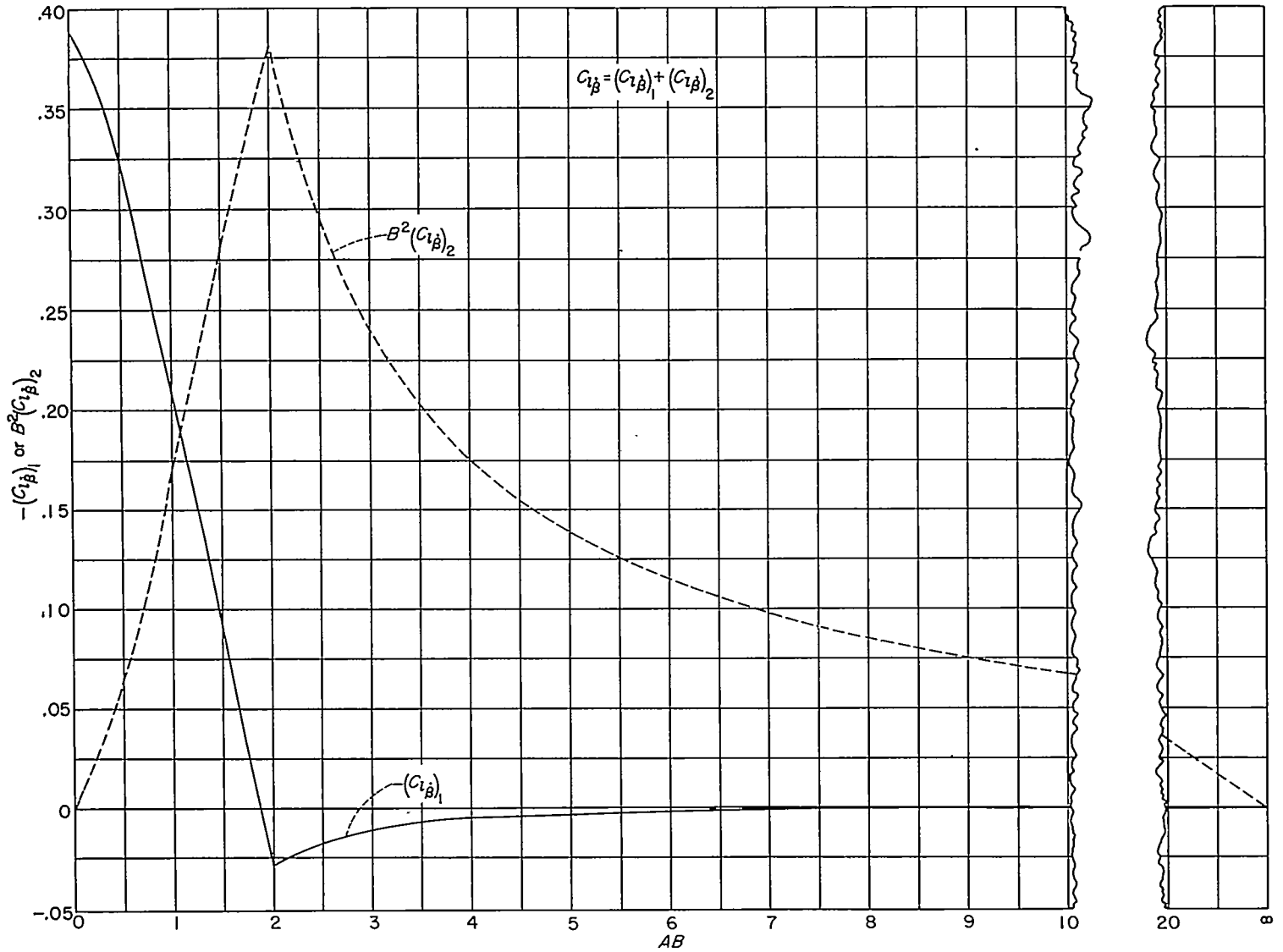
FIGURE 5.—Curves for determining the stability derivatives due to steady rolling C_{Y_p}, C_{n_p}, and C_{l_p} for isolated half-delta vertical tails. Derivatives based on vertical-tail parameters b, S, and angle pb/V; principal body-axes system with origin at leading edge of root section.
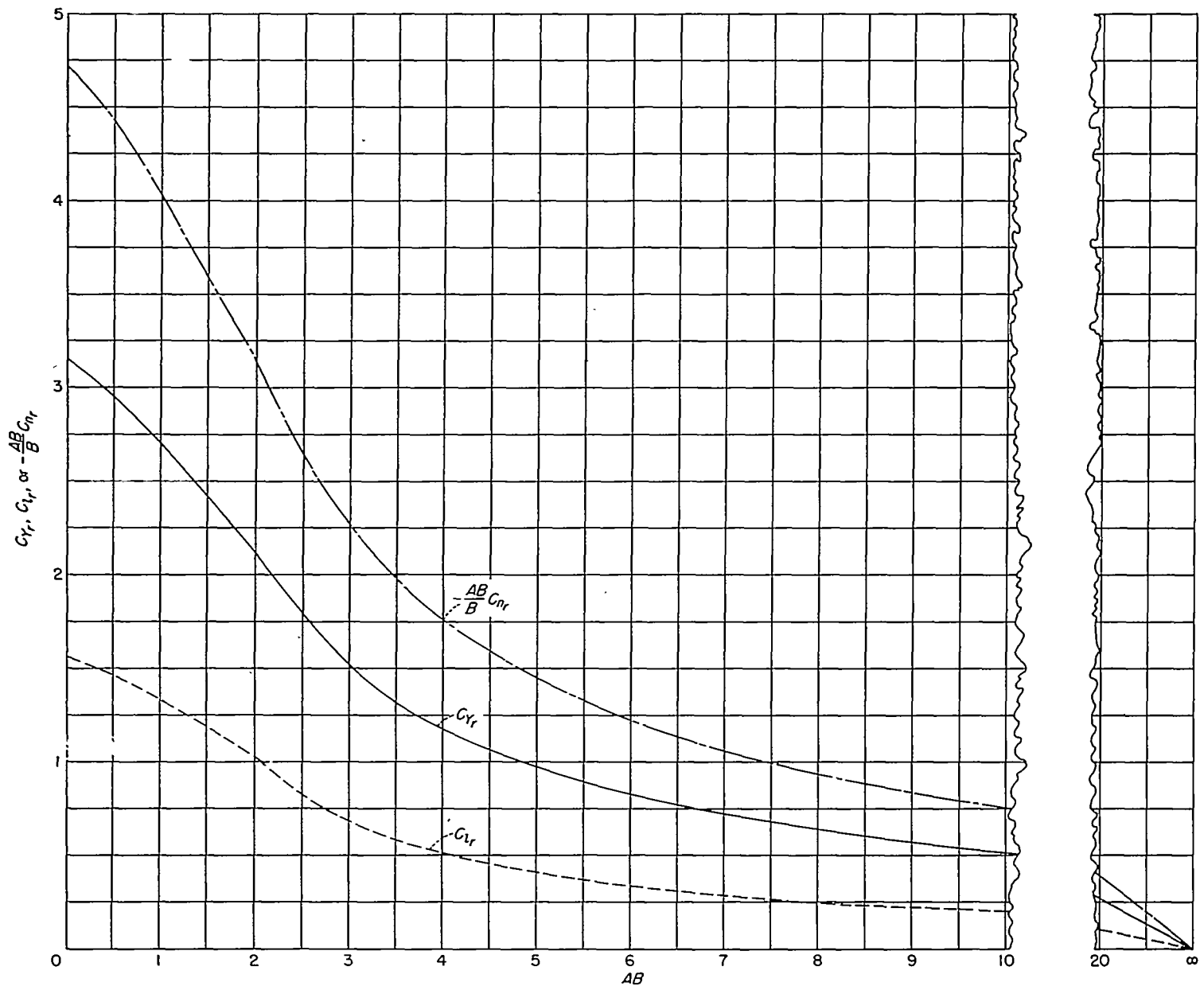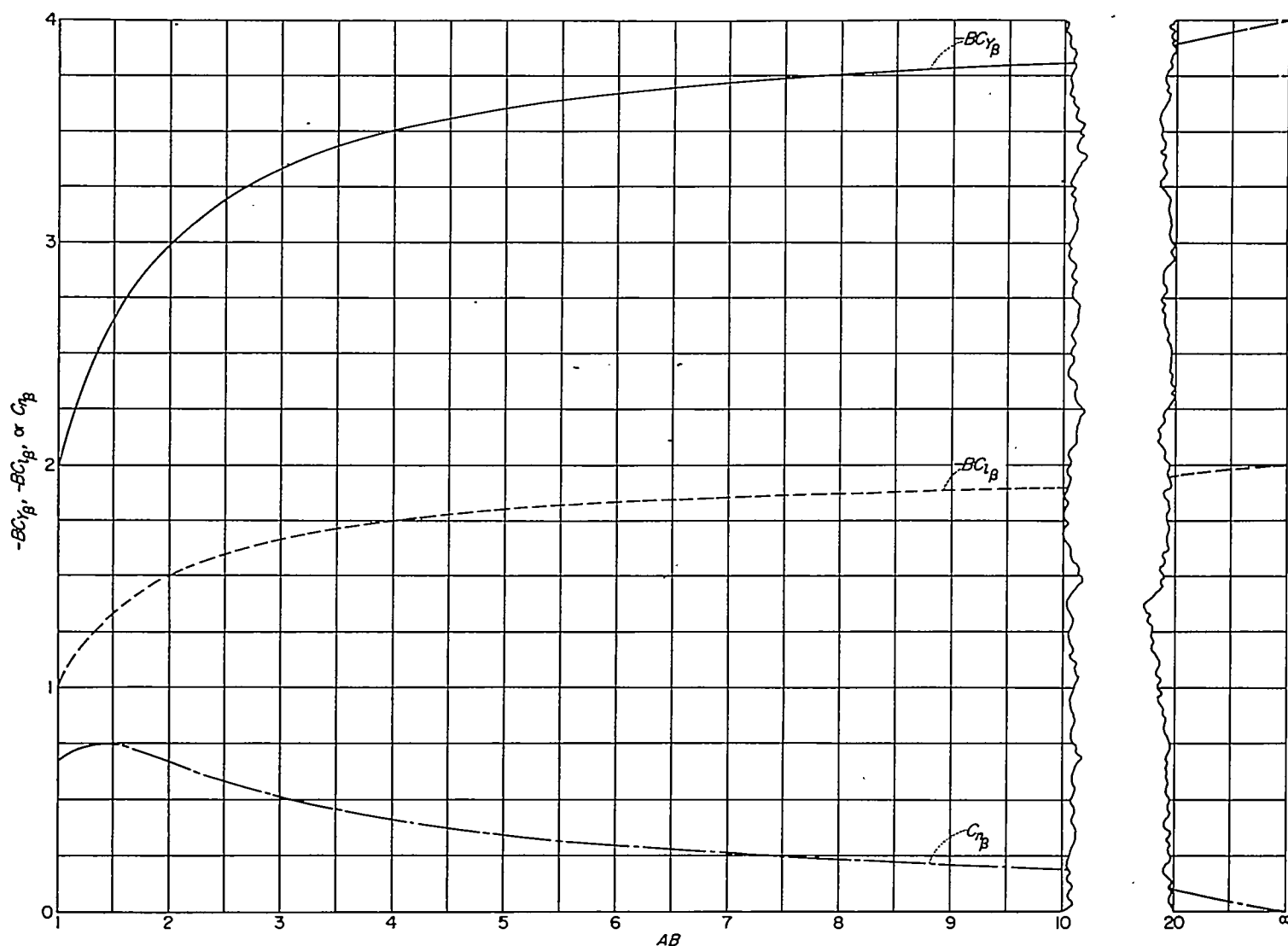
FIGURE 6.—Curves for determining the stability derivatives due to steady yawing C_{Y_r}, C_{n_r}, and C_{l_r} for isolated half-delta vertical tails. Derivatives based on vertical-tail parameters b, S, and angle rb/V; principal body-axes system with origin at leading edge of root section.
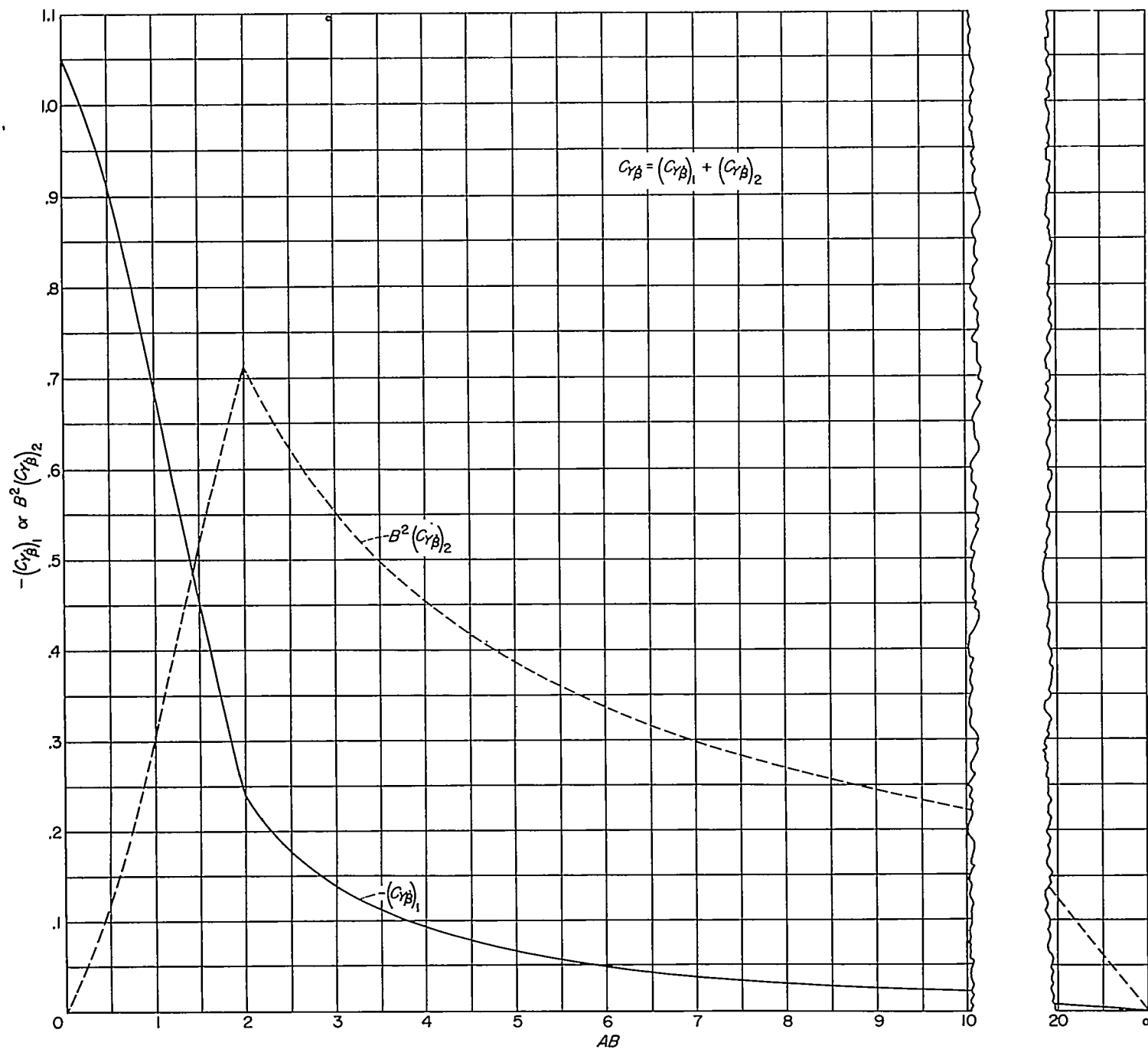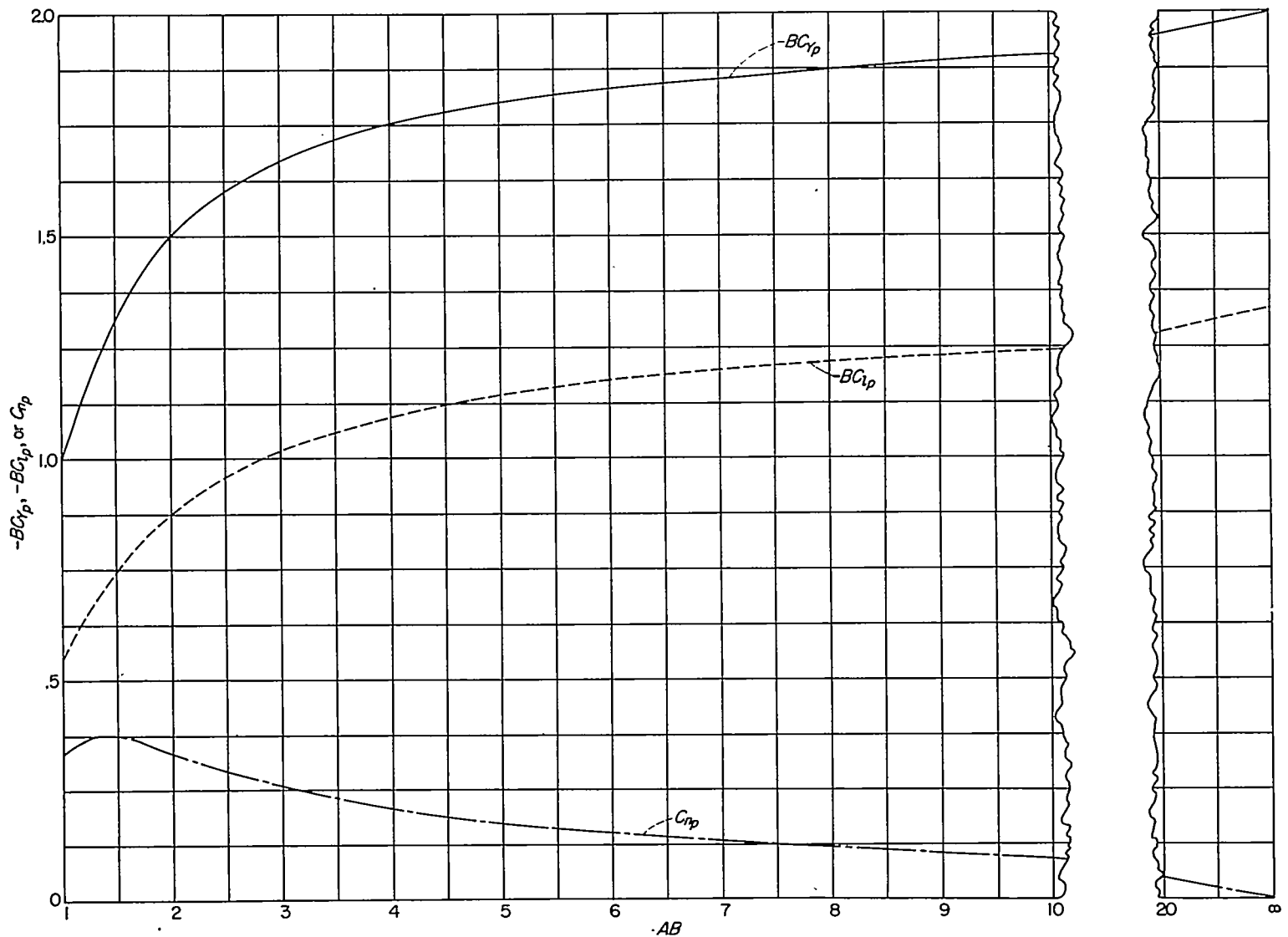
FIGURE 7.—Curves for determining the stability derivative due to constant lateral acceleration $C_{Y_{\dot{\beta}}}$ for isolated half-delta vertical tails. Derivative based on vertical-tail parameters b, S, and angle $\beta b/V$; principal body-axes system.

FIGURE 8.—Curves for determining the stability derivative due to constant lateral acceleration $C_{n_{\dot{\beta}}}$ for isolated half-delta vertical tails. Derivative based on vertical-tail parameters b, S, and angle $\beta b/V$; principal body-axes system with origin at leading edge of root section.
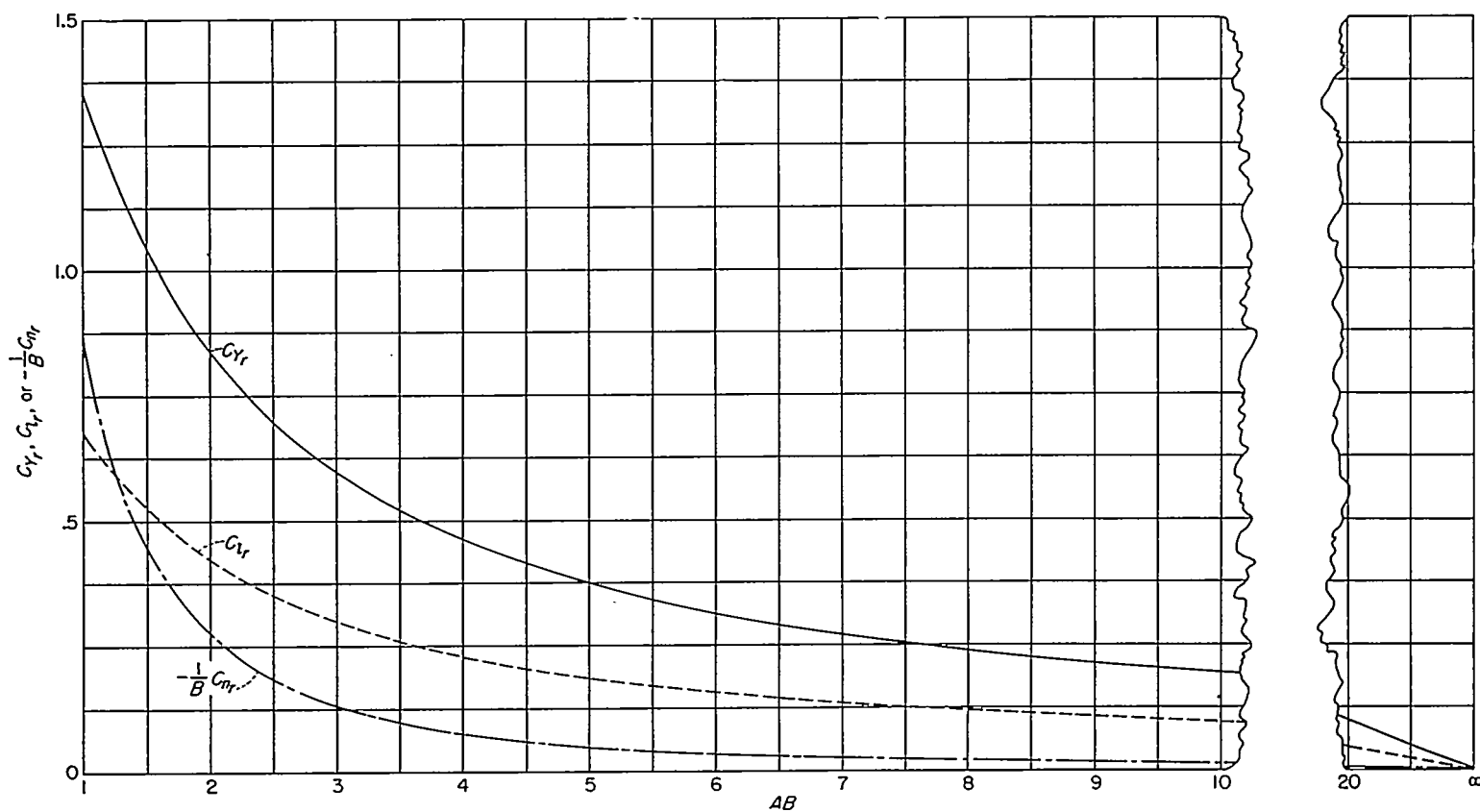
FIGURE 9.—Curves for determining the stability derivative due to constant lateral acceleration $C_{l_{\dot{\beta}}}$ for isolated half-delta vertical tails. Deriva. tive based on vertical-tail parameters b, S, and angle $\beta b/V$; principal body-axes system with origin at leading edge of root section.
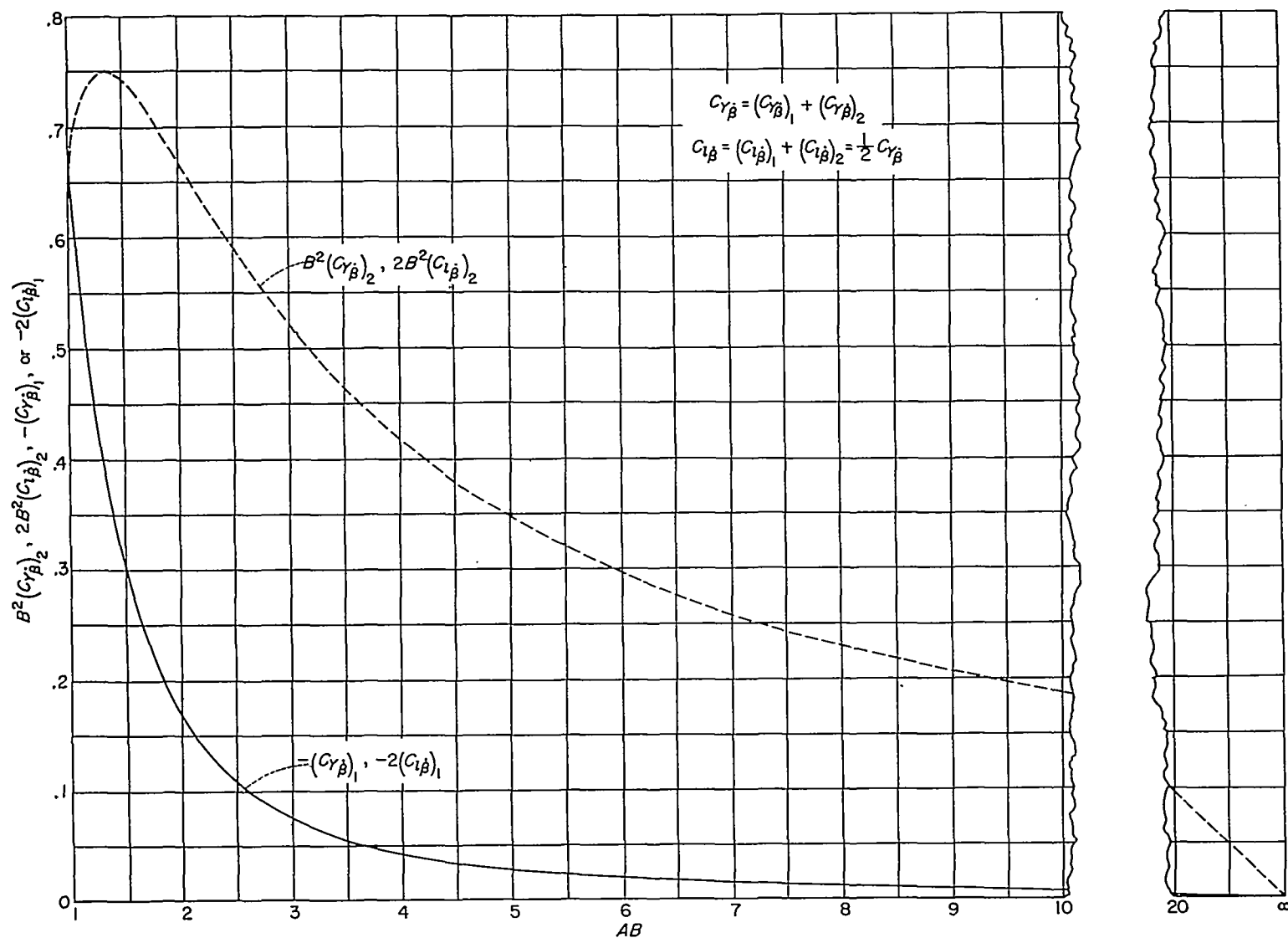
FIGURE 10.—Curves for determining the stability derivatives due to constant sideslip C_{Y_β}, C_{n_β}, and C_{l_β} for isolated rectangular vertical tails. Derivatives based on vertical-tail parameters b and S; principal body-axes system with origin at leading edge of root section.

FIGURE 11.—Curves for determining the stability derivatives due to steady rolling C_{Y_p}, C_{n_p}, and C_{l_p} for isolated rectangular vertical tails. Derivatives based on vertical-tail parameters b, S, and angle pb/V; principal body-axes system with origin at leading edge of root section.
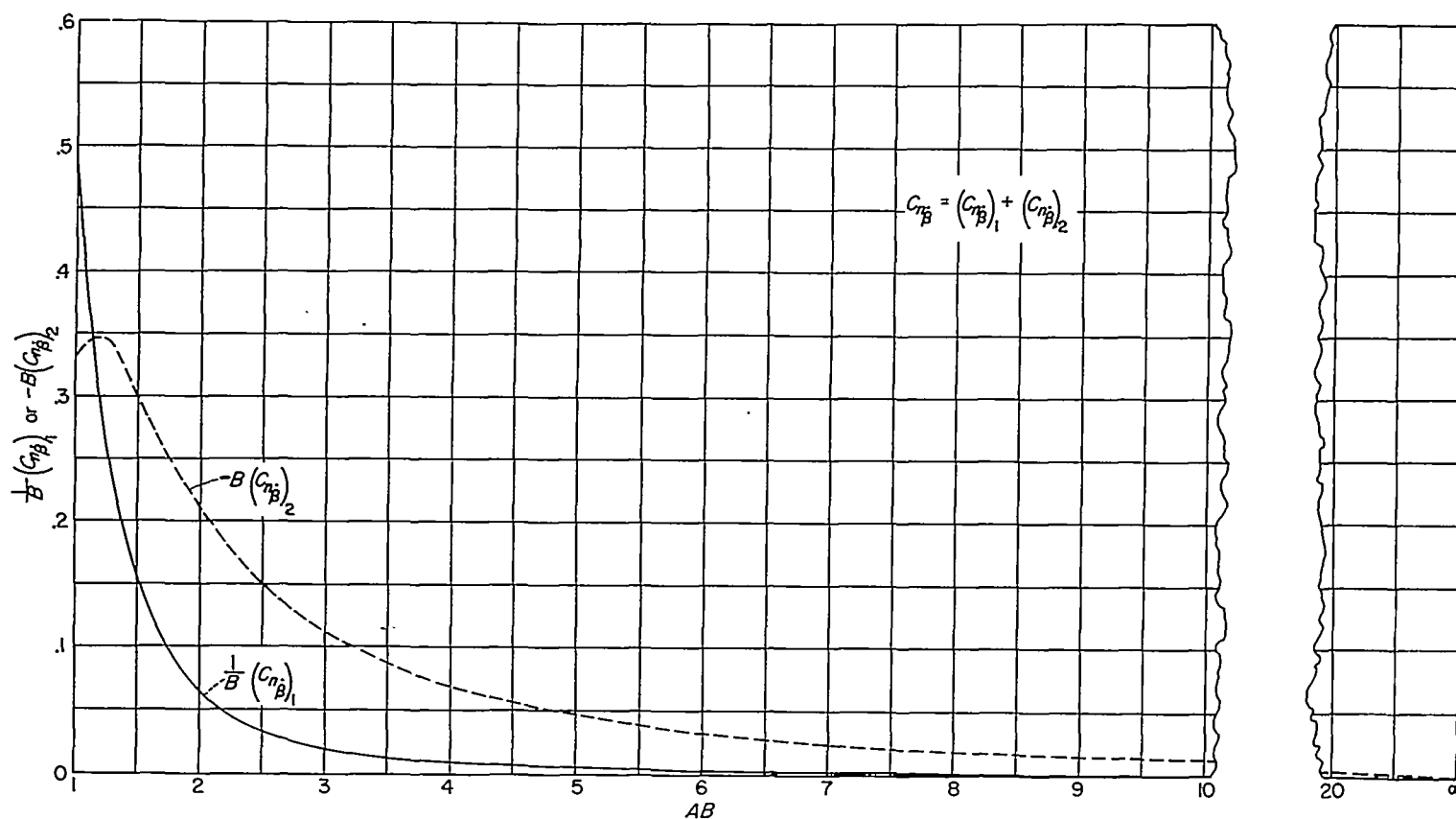
FIGURE 12.—Curves for determining the stability derivatives due to steady yawing C_{Y_r}, C_{n_r}, and C_{l_r} for isolated rectangular vertical tails. Derivatives based on vertical-tail parameters b, S, and angle rb/V; principal body-axes system with origin at leading edge of root section.

FIGURE 13.—Curves for determining the stability derivatives due to constant lateral acceleration $C_{Y_{\dot{\beta}}}$ and $C_{l_{\dot{\beta}}}$ for isolated rectangular vertical tails. Derivatives based on vertical-tail parameters b, S, and angle $\dot{\beta}b/V$; principal body-axes system with origin at leading edge of root section.

FIGURE 14.—Curves for determining the stability derivative due to constant lateral acceleration $C_{n_{\dot\beta}}$ for isolated rectangular vertical tails. Derivative based on vertical-tail parameters b, S, and angle $\beta b/V$; principal body-axes system with origin at leading edge of root section.
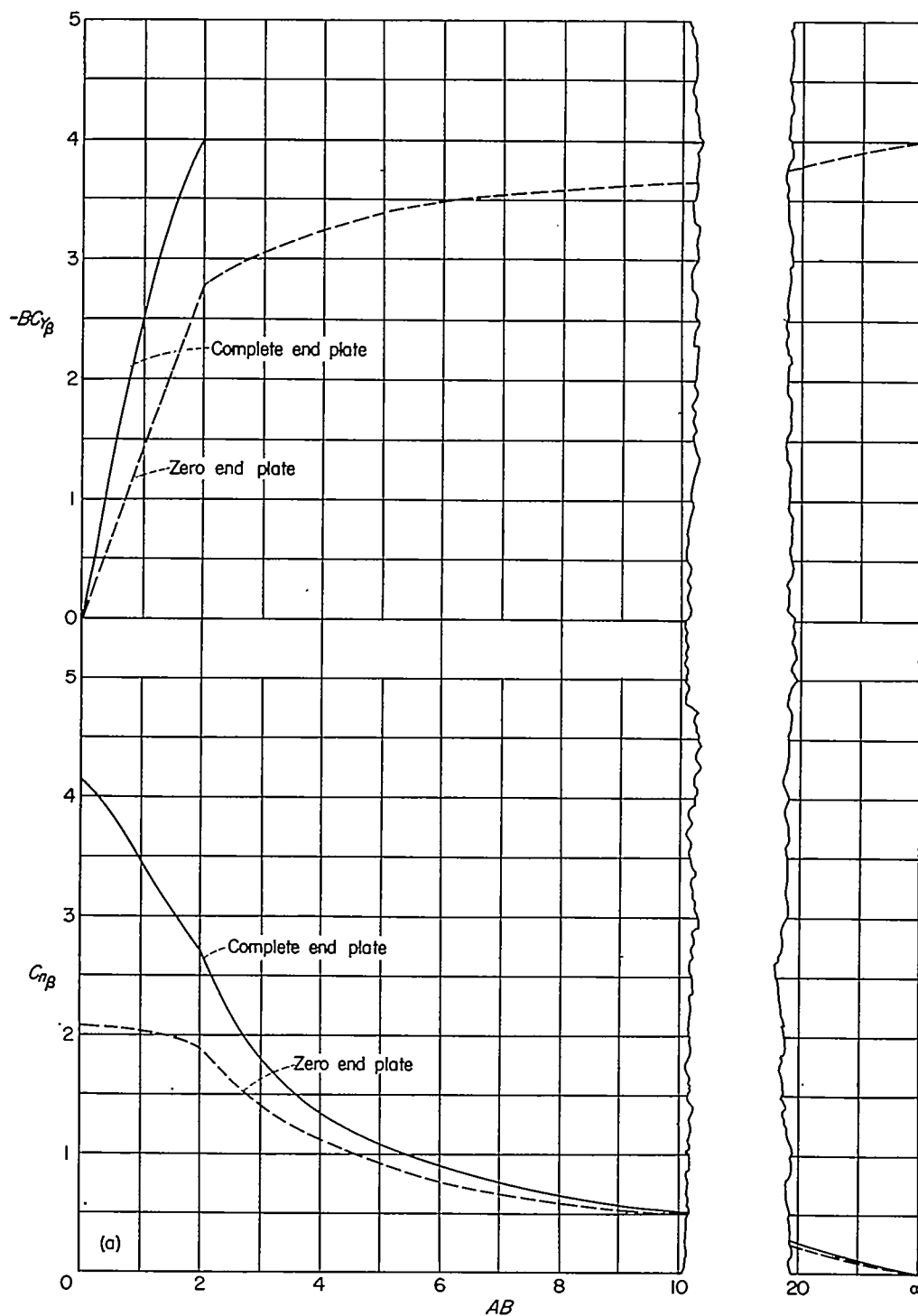
(a) Constant sideslip.

FIGURE 15.—Comparisons of zero- and complete-end-plate solutions for the side-force and yawing-moment derivatives due to several lateral motions for half-delta vertical tails. Derivatives based on vertical-tail parameters b, S, and angles pb/V, rb/V, and $\beta b/V$; principal body-axes system with origin at leading edge of root section.
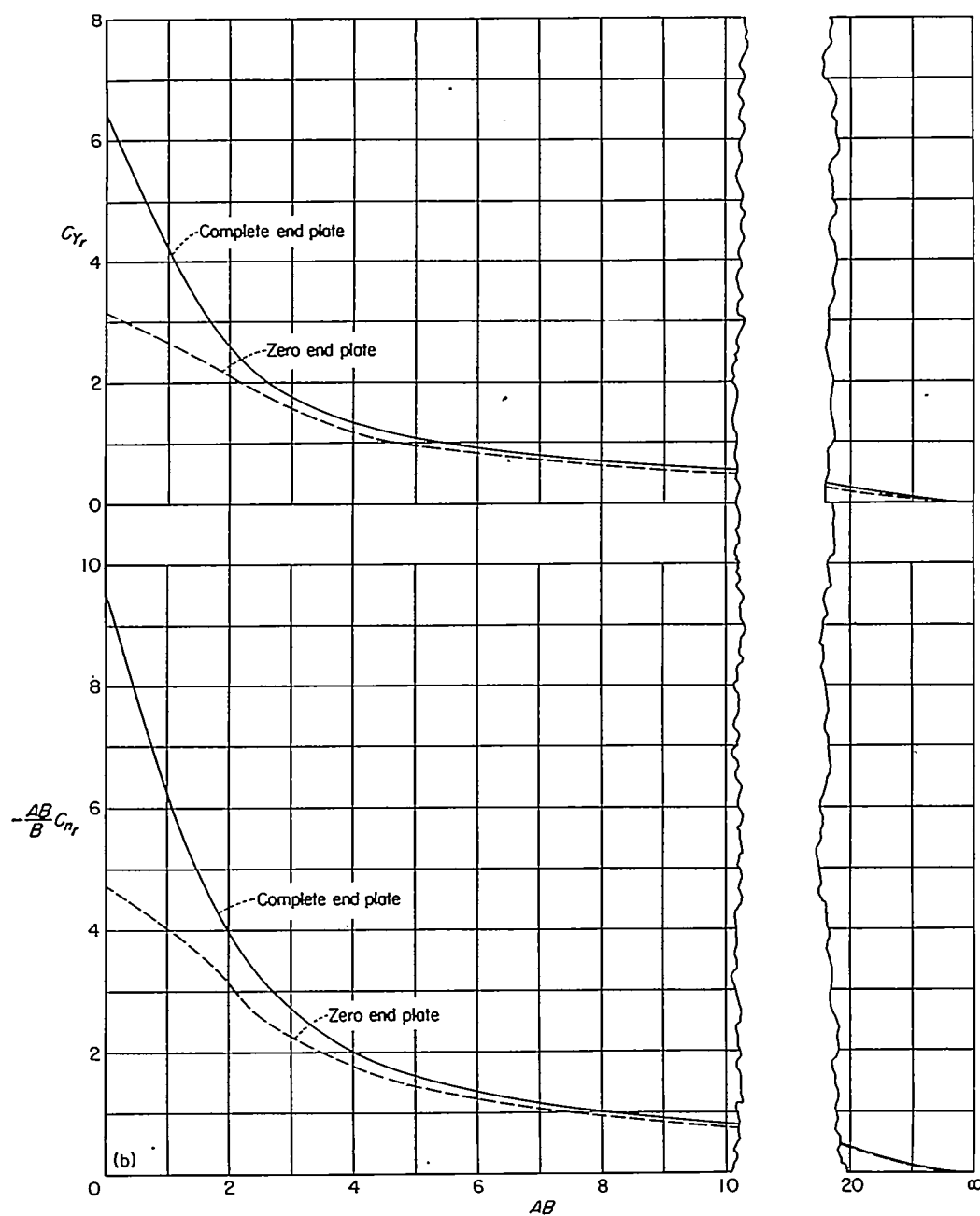
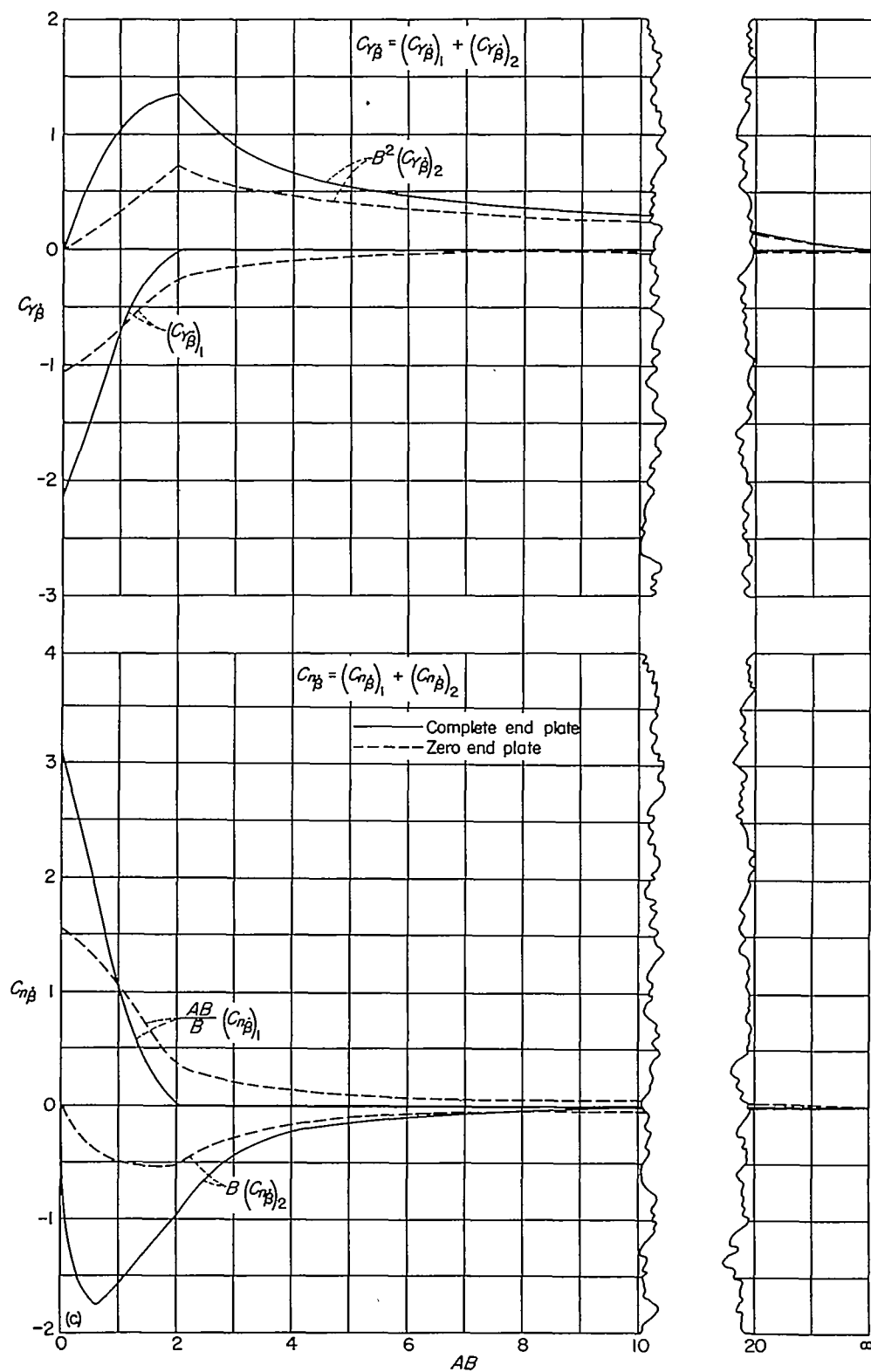(b) Steady yawing.

FIGURE 15.—Continued.
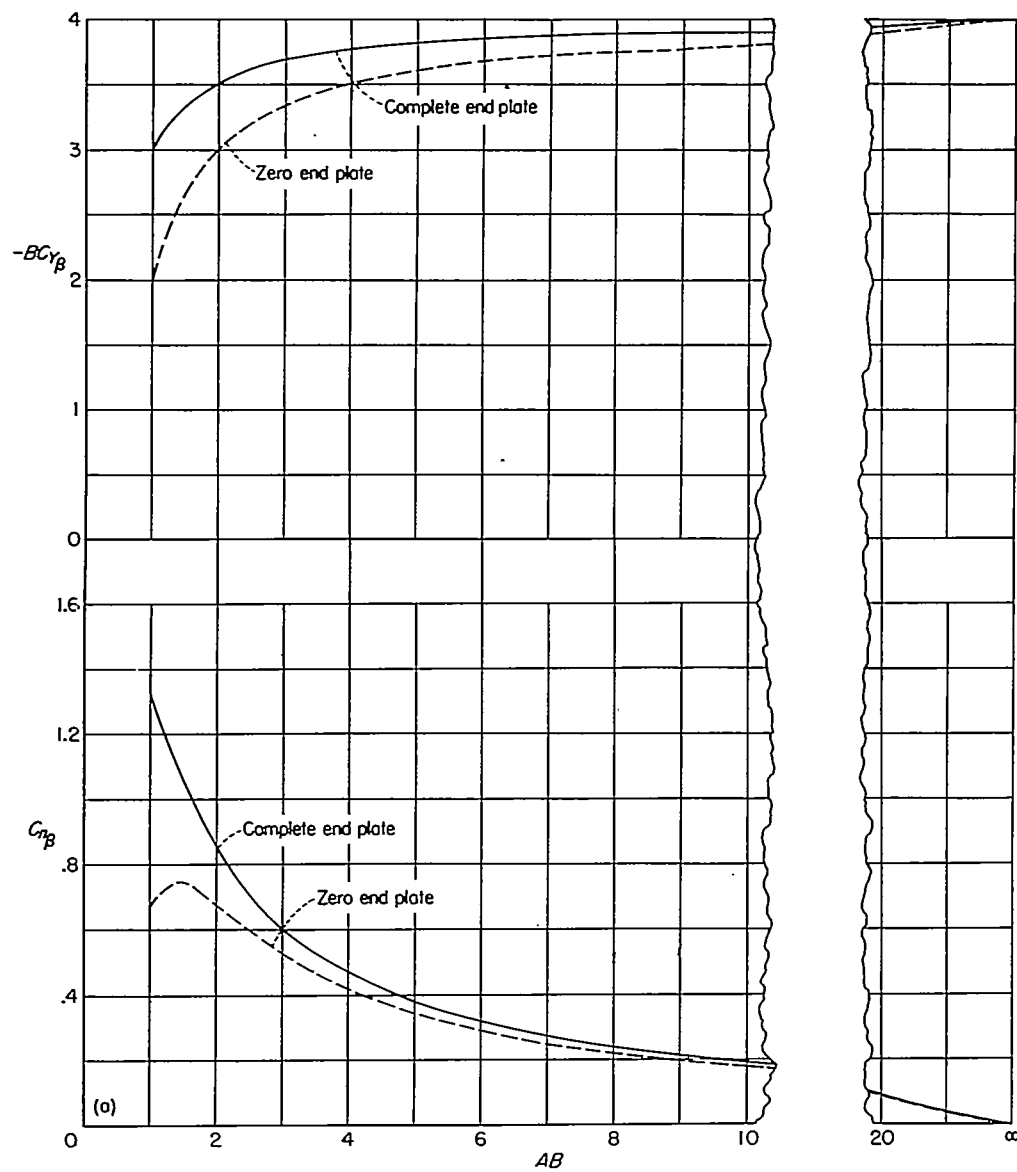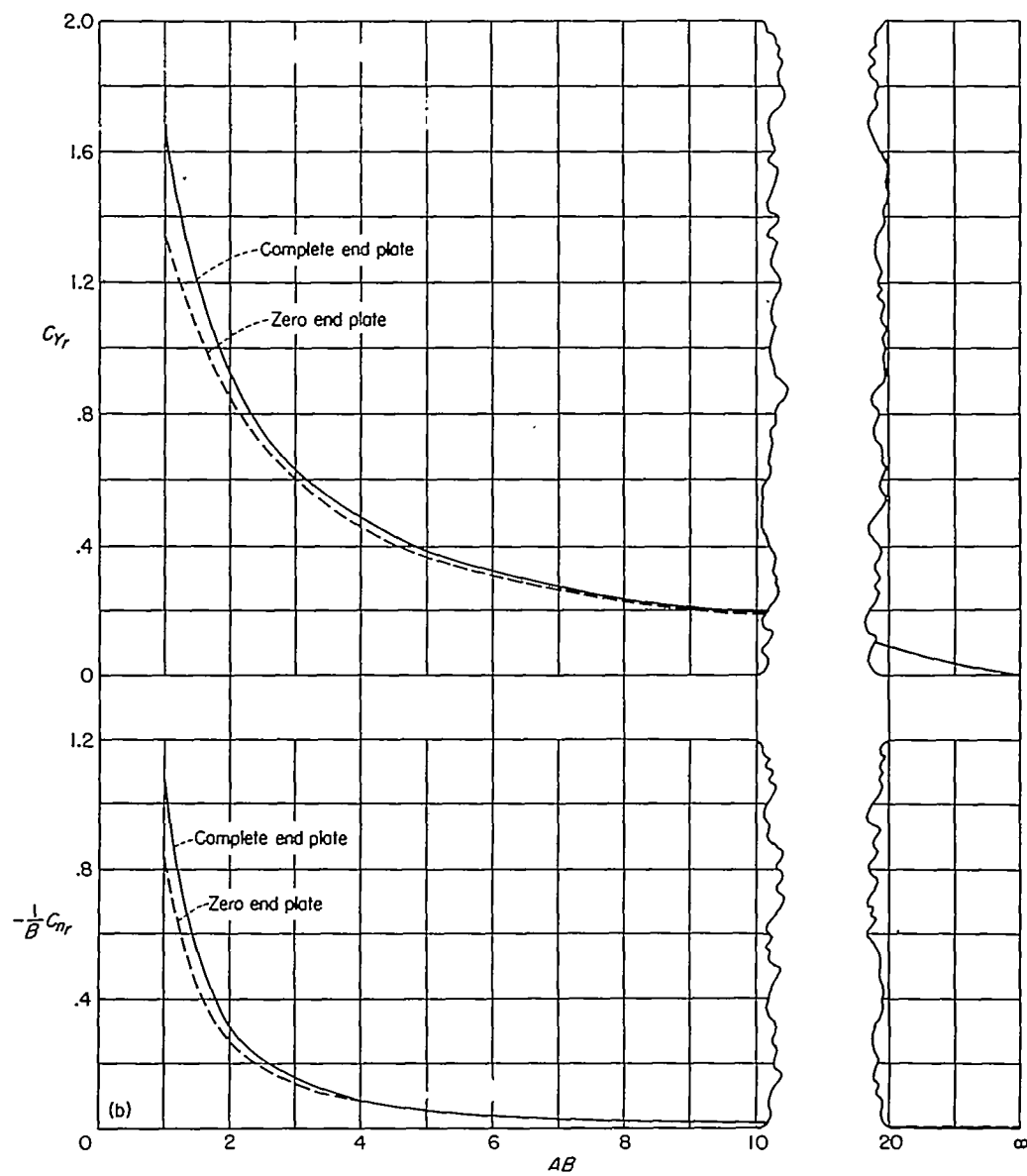
(c) Constant lateral acceleration.
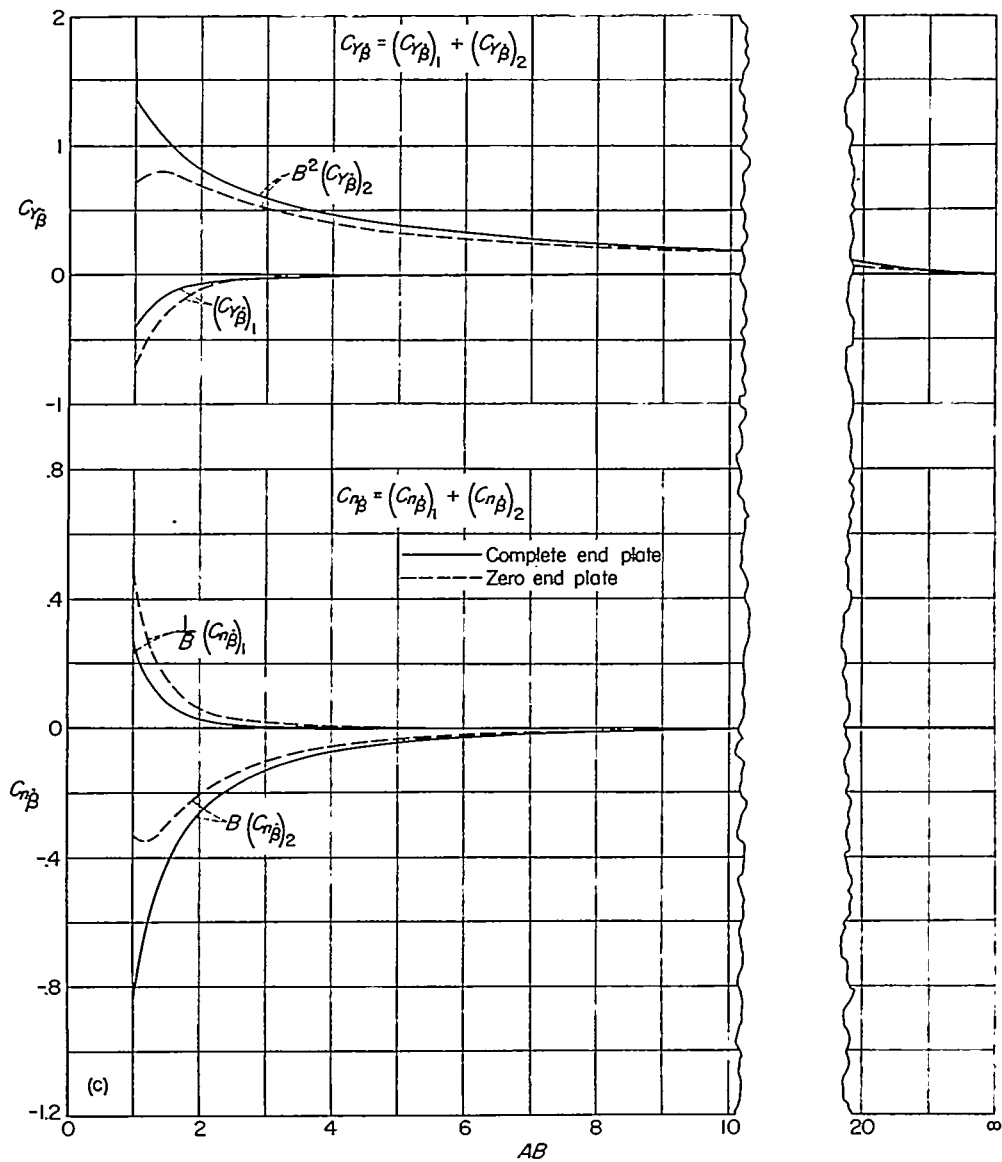
FIGURE 15.—Concluded.

(a) Constant sideslip.

FIGURE 16.—Comparisons of zero- and complete-end-plate solutions for the side-force and yawing-moment derivatives due to several lateral motions for rectangular vertical tails. Derivatives based on vertical-tail parameters b, S, and angles pb/V, rb/V, and $\beta b/V$; principal body-axes system with origin at leading edge of root section.

(b) Steady yawing.

FIGURE 16.—Continued.

(c) Constant lateral acceleration.

FIGURE 16.—Concluded.